공학석사 학위논문

Development of Reliability-Based Serviceability Limit State Design Method for Spread Foundations Under Uplift Loading in Cohesionless Soils

사질토지반에서 인발하중을 받는 확대기초의
신뢰성기반 사용성한계상태 설계법 개발

2023 년 2 월

서울대학교 대학원
건설환경공학과
한 재 인

Development of Reliability-Based Serviceability Limit State Design Method for Spread Foundations Under Uplift Loading in Cohesionless Soils

사질토지반에서 인발하중을 받는 확대기초의

신뢰성기반 사용성한계상태 설계법 개발

지도 교수 김 성 렬

이 논문을 공학석사 학위논문으로 제출함
2023 년 1 월

서울대학교 대학원
건설환경공학과
한 재 인

한재인의 공학석사 학위논문을 인준함
2023 년 1 월

위 원 장 ______정 충 기______ (인)

부위원장 ______김 성 렬______ (인)

위 원 ______박 준 범______ (인)

Abstract

Development of Reliability-Based Serviceability Limit State Design Method for Spread Foundations Under Uplift Loading in Cohesionless Soils

Han, Jayne
Civil & Environmental Engineering
The Graduate School
Seoul National University

The design of foundations is often governed by the serviceability limit state (SLS) requirements of the supported structure, particularly for large spread foundations. This paper aims to develop a reliability-based SLS design method for spread foundations under uplift loading in cohesionless soils. A probabilistic framework was adopted for the empirical characterisation of the compiled load-displacement curves and the quantification of the associated uncertainties. By using the obtained statistics of the curves, reliability analysis was carried out with Monte-Carlo simulations to calibrate the resistance factors within the load and resistance factor design (LRFD) framework. The calibration results showed that the embedment ratio of the foundation and the fitting errors of the empirical model, which were previously unaddressed in the literature, had notable effects on the calibrated SLS resistance factors. The relationship of the SLS with the ultimate limit state was assessed, including the governing limit state at each allowable displacement level, and the probability of ultimate failure of the foundation at the SLS condition. By considering the relationship between the limit states, the procedures for determining the design resistance factor and foundation capacity were proposed.

Keyword : serviceability limit state; reliability-based design; spread foundation; uplift; foundation engineering; LRFD; statistics

Student Number : 2021-28916

Table of Contents

List of Figures

List of Tables

Notations

Abbreviations

AASHTO	American Association of State Highway and Transportation Officials
AIC	Akaike Information Criterion
ASD	Allowable Stress Design
ASCE	American Society of Civil Engineers
BIC	Bayes Information Criterion
BS	British Standards
COV	Coefficient of Variation
DL	Dead Loads
EPRI	Electric Power Research Institute
FHWA	Federal Highway Administration
FORM	First Order Reliability Method
FOSM	First Order Second Moment
IEC	International Electrotechnical Commission
IEEE	Institute of Electrical and Electronics Engineers
LL	Live Loads
LRFD	Load and Resistance Factor Design
LSD	Limit State Design
MATLAB	Matrix Laboratory
MCMC	Markov Chain Monte Carlo
MCS	Monte Carlo Simulation
MPP	Most Probable Point
MvCAT	Multivariate Copula Analysis Toolbox
NCHRP	National Cooperative Highway Research Program
NESC	National Electrical Safety Code®
RBD	Reliability-Based Design
RBSLS	Reliability-Based Serviceability Limit State

RMSE	Root Mean Square Error
SHRP	Strategic Highway Research Program
SLS	Serviceability Limit State
SR	Settlement Ratio
ULS	Ultimate Limit State
WL	Wind Loads

Symbols

A	Area of the foundation base
a_i, b_i	Best fit coefficients of the regression function
B	Foundation width
B'	Equivalent foundation width
c	Cohesion of the soil
D	Foundation embedment depth
D/B	Ratio of the foundation depth to width
E_s	Elastic modulus of the soil
F	Frictional forces that act along the uplift failure surface
f_i, f_1, f_2	Regression function used to remove the statistical dependency
g	Performance function or failure function
H	Limiting value of the failure surface depth
H/B	Limiting embedment ratio
I	Indicator function
I_p	Displacement influence coefficient
K	Horizontal earth pressure coefficient
k	Shape parameter
K_u	Nominal uplift coefficient of earth pressure
L	Foundation length
M	Coefficient for the computation of the shape factor
M_{fit}	Fitting model factor
M_{SLS}	Serviceability limit state model factor
M_{ULS}	Capacity model factor of the ultimate capacity of the foundation

M^{*}_{ULS}	Capacity model factor of the interpreted capacity of the foundation
N	Number of data points
N_{s}	Number of simulations
P	Foundation perimeter
$P(\cdot)$	Probability of occurrence
p	Spearman's p-value
p_{f}	Probability of failure
Q, Q_i	Load
Q_{all}	Allowable load
Q_{app}	Uplift loads applied to the foundation
Q_{d}	Design capacity of the foundation
Q_{DL}	Dead loads
Q_{fitted}	Predicted load from the fitted curves
$Q_{i,\mathrm{n}}$	Nominal load
Q_{max}	Maximum value of the normalised load
Q_{measured}	Measured load
Q_{ref}	Reference capacity
Q_{TIU}	Tangent intersection capacity
Q_{u}	Ultimate uplift capacity of the foundation
$Q_{\mathrm{u,int}}$	Interpreted capacity of the foundation
Q_{uc}	Predicted ultimate capacity of the foundation
Q_{WL}	Wind loads
$Q_{0.01\mathrm{B}}$	Slope tangent capacity with the offset of 0.01 times the foundation width
$Q_{0.02\mathrm{B}}$	Slope tangent capacity with the offset of 0.02 times the foundation width
R	Resistance of the structure
R_{n}	Nominal resistance
s_{f}	Shape factor
W_{f}	Weight of the foundation
W_{s}	Weight of soil in the failure surface above the foundation slab
Y	Horizontal distance between the foundations
$\hat{y}_i$	Predicted value from the empirical model

y_i	Measured value
α	Copula parameter
β	Reliability index
β_{SLS}	Reliability index for serviceability limit state design
β_T	Target reliability index
β_{ULS}	Reliability index for ultimate limit state design
γ_s	Unit weight of soil
γ, γ_i	Load factor
γ_{DL}	Load factor for dead loads
γ_{WL}	Load factor for wind loads
δ	Displacement
δ_{all}	Allowable displacement
$\delta_{calculated}$	Calculated displacement
$\delta_{measured}$	Measured displacement
η	Pseudo-strain
η_{all}	Allowable pseudo-strain
η_i	Load modifier
η_{lim}	Limiting pseudo-strain
θ_1, θ_2	Empirical fitting coefficients of the hyperbolic model
$\theta_{1,t}$, $\theta_{2,t}$	Treated fitting coefficients of the hyperbolic model
θ_3, θ_4	Empirical fitting coefficients of the power law model
λ	Bias
μ	Mean
ρ	Pearson correlation coefficient
ρ_τ	Kendall's tau coefficient
$\rho_{\tau,sim}$	Simulated Kendall's tau coefficient
ϕ	Friction angle of the soil
$\Phi(\cdot)$	Standardised normal distribution function
ψ	Resistance factor
ψ_d	Design resistance factor
ψ_{SLS}	Resistance factor for serviceability limit state design
ψ_{ULS}	Resistance factor for ultimate limit state design
ω	Ratio of wind loads to dead loads

Chapter 1. Introduction

1.1. Background

The design of foundations involves uncertainties that arise from various sources, such as the natural variability of the soil properties, and the model uncertainties that are caused by the assumptions in the calculation models. To address these uncertainties and the associated risks, reliability-based design (RBD) methods have been developed and implemented in several design codes, including the AASHTO LRFD Bridge Design Specifications [1], the Canadian Highway Bridge Design Code [2], and Eurocode 7 [3]. In the RBD of foundations, the probability of the foundation reaching the ultimate limit state (ULS) or the serviceability limit state (SLS) is assessed.

Specifically in the context of spread foundations for light-weight lattice structures such as transmission and telecommunication towers, the limit states are governed by the uplift behaviour of the foundation [4], [5]. The applied uplift forces are induced by the overturning effects that are caused by the horizontal loads acting on the supported structure, including wind loads. The resulting displacements and differential settlements of the foundation system can lead to deformations and potential failure in the supported structure [4], [6], [7], which may be a more crucial consideration than foundation failure [8]. Particularly for large spread foundations, the design is often governed by the serviceability requirements of the supported structure, due to their high susceptibility to significant displacements before failure [9], [10]. This entails the need to develop reliability-based serviceability limit state (RBSLS) design methods for spread foundations under uplift loading. However, up to date, there have been limited development and evaluation of the RBSLS design methods for this specific design condition.

Overall, previous research suggested two main approaches for developing RBSLS design methods. The first approach is to quantify the uncertainties in the foundation displacement by assessing the probability distribution characteristics of the displacement model factor, defined as the ratio of the measured displacement value to the predicted value at a given load [11]–[14]. While this is consistent with the approach for the reliability-based ULS design methods, this approach cannot be applied to design conditions that have no relevant prediction models. Such limitations apply to the design of spread foundations under uplift loading, which do not have generalised prediction models for the uplift displacement [4]. To overcome this shortcoming, recent studies have developed the second approach of assessing the statistical characteristics of the load-displacement curves by modelling the curves as an empirical bi-variate model [15]–[17]. The obtained statistical characteristics are used to simulate the overall load-displacement behaviour of the foundation, allowing for an estimation of the foundation reliability over a wide range of displacements. This approach has been widely applied to various types of foundations and design conditions which do not have available prediction models, such as augured cast-in-piles in granular soils under compression [18], and helical anchors in clays under uplift loading [19].

While the approach of using an empirical model has also been applied by Tang et al. [20] and the EPRI TR-105000 report [21] for spread foundations under uplift loading, several considerations were not addressed in these studies. For instance, the errors between the fitted empirical curves and the actual measurements were not considered, although discrepancies may be present. Also, the statistical dependencies in the parameters of the empirical model were not checked, which implies that the parameters were assumed to be random variables. Thus, there is the need to incorporate such considerations to improve the accuracy of the RBSLS development procedures.

In addition, there has been limited evaluation of the relationship between the foundation reliability against two limit states (ULS and SLS), as the majority of studies focussed on individual assessments of each limit state. Some studies have investigated the relationship between the limit states by assessing the governing limit state for design, based on the designed foundation width and load capacity [9], as well as the reliability of the foundation at the ULS and SLS for varying serviceability requirements (i.e. allowable displacement) [22]. Overall, it was shown that the SLS governs the design for a specific range of design conditions only (e.g. foundations with large widths); however, such conditions are not explicitly incorporated into the current RBSLS design procedures.

1.2. Purpose of Research

The main objective of this research is to develop the RBSLS design method for spread foundations under uplift loading in cohesionless soils by adopting the framework of using an empirical bi-variate model to characterise the statistics of the uplift load-displacement curves. Previously unaddressed sources of uncertainties and statistical dependencies were identified and incorporated into the analysis, in order to improve the accuracy of the estimated foundation reliability and the reliability analysis outputs. This includes the fitting errors between the measured and fitted load-displacement curves, and the statistically significant dependencies between the model fitting coefficients and the foundation design parameters. Moreover, this research aims to investigate the relationship between the SLS and ULS for its incorporation into the RBSLS design procedures.

1.3. Outline of This Study

This research characterises the uplift load-displacement behaviour of the foundation and its statistical characteristics to evaluate the foundation reliability against the SLS, and proposes an updated RBSLS procedure that considers the relationship between the ULS and SLS. In Chapter 2 of this study, a literature review was conducted to outline the concept of limit state design and reliability-based design methods, as well as the previous approaches for developing the RBSLS design methods. Based on the literature review, the current limitations about the RBSLS design of spread foundations under uplift loading were identified.

Chapter 3 describes the details of the procedures for characterising the statistics of the compiled load-displacement curves via the use of an empirical bi-variate model. In this chapter, the database of 61 load-displacement curves was compiled and analysed to quantify the uncertainties in the uplift behaviour of spread foundations. Different empirical models and normalisation protocols were compared to identify the optimal option that gives the least scatter in the curves. The statistical dependencies in the fitting coefficients were treated, and the probability distributions of the treated fitting coefficients were obtained. The dependencies between the coefficients were characterised by using copula theory, which is suitable for defining nonlinear correlations between multiple variables.

In Chapter 4, reliability-based calibrations were carried out via Monte-Carlo simulations (MCS) within the context of transmission tower foundations with the quantified characteristics of the load-displacement curves. Based on the calibration results, the relationship between the reliability of the foundation at the SLS and ULS was assessed to determine the conditions where the SLS becomes the governing limit state, and to estimate the probability of the foundation reaching ultimate failure at a given SLS design criterion.

In Chapter 5, the RBSLS design procedures were proposed by incorporating the obtained resistance factors and the relationship between the two limit states. A design example was provided to demonstrate the use of the proposed design procedures. Chapter 6 provides a summary of the conclusions and recommendations for further work. Appendix A presents the detailed database of uplift load tests on spread foundations under uplift loading in cohesionless soils, which was used in this study. Appendix B shows the convergence test that was carried out to check whether the number of data in the database is sufficient for the purpose of this study.

Chapter 2. Literature Review

2.1. Introduction

The failure condition of the foundation can be defined with two types of limit states, the ultimate limit state (ULS) and the serviceability limit state (SLS) [23]. To date, the main focus has been placed on the reliability-based ULS design, which assesses the probability of the applied loads exceeding the ultimate failure capacity of the foundation. Reliability-based ULS design methods have already been implemented in several limit state design codes that are used in practice [1]–[3]. Although relatively limited, reliability-based serviceability limit state (RBSLS) design has recently been receiving increasing attention in the literature [9], [13], [15], [17], [24].

This chapter reviews the concepts of limit state design, and its application in the design of spread foundations under uplift loading in cohesionless soils. The concepts of RBD have been reviewed, along with different reliability analysis methods that were adopted for the estimation of the foundation reliability. An overview of the RBSLS development framework is provided, with focus on the characterisation of the uncertainties in the load-displacement relation of the foundation. The literature review is concluded with a summary and a discussion of the limitations of the current RBSLS design of spread foundations subjected to uplift loading.

2.2. Limit State Design (LSD)

The limit state is defined as the state "beyond which the structure no longer fulfils the relevant design criteria" and its intended function [25], [26]. The structure is considered to be in a condition near failure if the limit state is reached. The limit state design (LSD) comprises the procedures of identifying all possible failure mechanisms and limit states of the structure, and checking the design of the structure for each limit state [27]. For each structural component and limit state, the following equation is required to be satisfied [1]:

$$\sum \eta_i \gamma_i Q_{i,\mathrm{n}} \leq \psi R_\mathrm{n} \qquad \text{(Eq. 2.1)}$$

where η_i is the load modifier, γ_i (≥ 1) is the load factor applied to the nominal load $Q_{i,\mathrm{n}}$, ψ (≤ 1) is the resistance factor, and R_n is the nominal resistance.

By checking that the factored resistance is greater than the factored loads, it is ensured that the occurrence of the limit states is sufficiently improbable. Usually, the design of foundations is checked at two types of limit states, the ultimate limit state (ULS) and the serviceability limit state (SLS) [23]. The ULS is related to the structural safety and collapse of the structure, where the ultimate capacity of the foundation is exceeded by the applied loads. The SLS relates to the functionality of the structure, where the displacement, settlements, or distortions of the foundation exceed the allowable limits under the given loading conditions.

The following sections review the geotechnical calculation models and failure criteria for the ULS and SLS design of spread foundations under uplift loading in cohesionless soils.

2.2.1 Ultimate Limit State (ULS) Design

2.2.1.1 Calculation Models for the Uplift Capacity of Spread Foundations

Several calculation models (i.e. ULS models) are available for the estimation of the ultimate uplift capacity of spread foundations. The models can be applied to foundations with an enlarged base, including shallow foundations, grillage foundations, and anchors [5]. Overall, the calculation models consider different uplift failure mechanisms and failure surfaces that form in the soil beneath the ground surface. At the failure surface, the shear strength of the soil is assumed to be fully mobilised.

The types of calculation methods include the shear method, which assumes a vertical failure surface due to uplift, and the curved surface method which assumes a curved failure surface (Figure 2.1). Based on the assumed form of the failure surface, the ultimate uplift capacity of the foundation is calculated by summing the different force components that resist the uplift forces. The typical form of the prediction equation is as follows (Equation 2.2):

$$Q_u = W_f + W_s + F \quad \text{(Eq. 2.2)}$$

where Q_u is the ultimate uplift resistance or capacity of the foundation, W_f is the weight of the foundation, W_s is the weight of soil encapsulated by the failure surface, and F is the frictional forces that act along the failure surface.

Among various calculation methods, the IEEE [5] method and the Meyerhof and Adams [28] method have been widely used for the analysis of the uplift capacity of spread foundations [20], [29]–[31]. The IEEE method [5], proposed by Kulhawy et al. [4], is a type of shear method where the frictional force (F) in Equation 2.2 is calculated with Equation 2.3 for square and circular foundations.

$$F = cPD + \left(\frac{P}{2}\right) K \gamma_s D^2 \tan\phi \quad \text{(Eq. 2.3)}$$

where P is the foundation perimeter, D is the foundation embedment depth from the bottom of the foundation slab to the ground surface, c is the cohesion of the soil, ϕ is the friction angle of the soil, γ_s is the unit weight of soil, and K is the horizontal earth pressure coefficient.

While the IEEE [5] method is simple to apply, it does not consider the effects of embedment depth on the failure mode of the foundation. Several researchers have reported that the ratio of the foundation depth to width (D/B) influences the uplift failure mode of the foundation; for spread foundations that are embedded at a shallow depth, the failure surface extends to the ground surface, while for deeply embedded foundations, local failure occurs near the foundation base [29], [32], [33].

The Meyerhof and Adams [28] method is a curved surface method (Figure 2.2), which distinguishes the shallow and deep failure modes. The limiting value of D/B that distinguishes the shallow and deep failure modes is expressed as the limiting embedment ratio (H/B), also known as the critical embedment ratio. Different equations have been suggested for shallow embedment depths of $D < H$, and deep embedment depths of $D \geq H$, as shown in Equation 2.4 for circular and square foundations.

$$Q_u = W_f + A\gamma_s D + cPD + s_f\left(\frac{P}{2}\right)\gamma_s D^2 K_u \tan\phi \qquad (D < H) \qquad \text{(Eq. 2.4a)}$$

$$Q_u = W_f + A\gamma_s H + cPH + s_f\left(\frac{P}{2}\right)\gamma_s H(2D - H) K_u \tan\phi \quad (D \geq H) \qquad \text{(Eq. 2.4b)}$$

where A is the foundation base area, H is the limiting value of the failure surface depth, K_u is the nominal uplift coefficient of earth pressure ($= 0.496\phi^{0.18}$), and s_f is the shape factor ($= 1 + \frac{MD}{B} \leq 1 + \frac{H}{B}M$). The values of H/B and M, required for the computation of the shape factor s_f, are obtained from Table 2.1.

For all calculation models, inherent errors and uncertainties are present, due to the simplification and assumptions that are made in the models [34]. Such errors can lead to an over-/underestimation of the foundation capacity, and the deviation between the predicted and actual capacity. Thus, it is necessary to evaluate and verify the calculation models through a comparison between the predicted capacity value and the actual value measured from load tests.

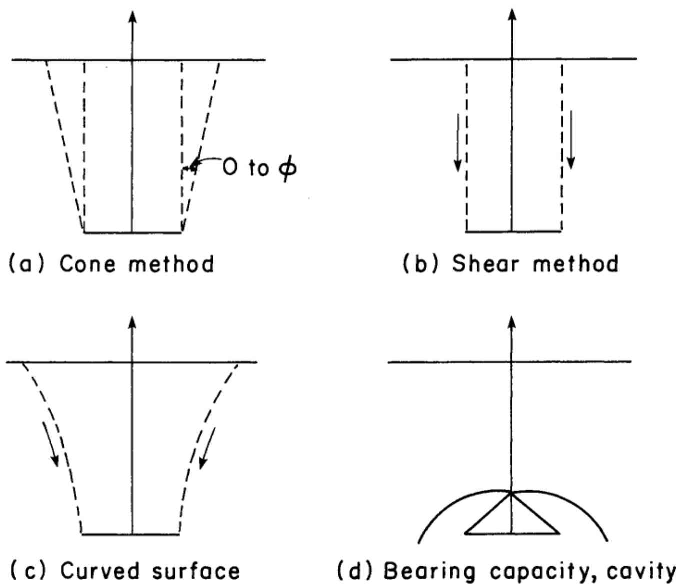

Figure 2.1 Types of uplift capacity models (Kulhawy et al. [4]).

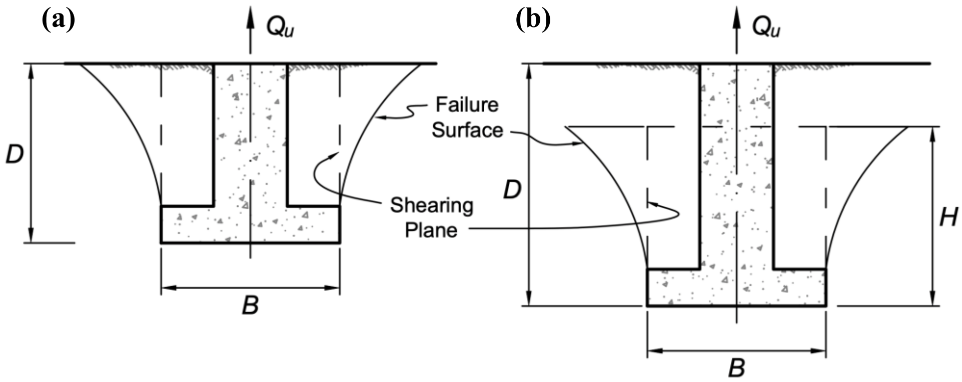

Figure 2.2 Uplift failure mechanism of spread foundations considered in the Meyerhof and Adams [28] method: (a) shallow foundations; and (b) deep spread foundations (Adapted from IEEE [5]).

Table 2.1 Values of *H/B* and *M* for the Meyerhof and Adams [28] method

ϕ (°)	20	25	30	35	40	45	48
H/B	2.5	3.0	4.0	5.0	7.0	9.0	11.0
M	0.05	0.10	0.15	0.25	0.35	0.50	0.60

2.2.1.2 Interpretation of the Uplift Capacity from Load Test Results

The actual value of the uplift capacity of foundations can be obtained through the analysis of the load test results. In the measured load-displacement (Q-δ) relation from the load test, a specific value is determined as the ultimate capacity of the foundation, which can be used to verify the predicted capacity value from the calculation models [4]. Table 2.2 summarises the failure criteria that have been applied for the interpretation of the uplift capacity of foundations.

Specifically in the EPRI EL-2870 [4] report, the tangent intersection method was selected for the determination of the uplift capacity of grillages, a type of spread foundation, while the slope tangent method with the offset of 0.15 in (4mm) was chosen for drilled shafts. While the study [4] illustrated that both methods give similar results for sharply turning load-displacement curves, each interpretation method was shown to have its own inherent limitations. For instance, the tangent intersection method is subjected to scale effects and human judgement [35], [36], and the determined capacity is highly sensitive to the gradient of the final linear section of the curve.

Depending on the interpretation method used, the magnitude and consistency of the defined failure load vary significantly; the interpretation method and failure criteria can directly affect the extent of deviation between the measured capacity and predicted foundation capacity obtained from the calculation models. Based on this, it is seen to be desirable to select an appropriate interpretation method, which gives a capacity value that closely approximates the estimated value.

2.2.2 Serviceability Limit State (SLS) Design

2.2.2.1 Calculation Models for the Uplift Displacement of Spread Foundations

Up to date, no generalised calculation models or theories have been specifically established for the prediction of the uplift displacement of spread foundations. It was suggested by Kulhawy et al. [4] that the cylindrical shear model, which was proposed by Witham and Kulhawy [37] for the uplift displacement of shaft-type foundations, could be applied to spread-type foundations as well. The uplift displacement δ is calculated as follows:

$$\delta = \frac{(Q_\mathrm{u} - W_\mathrm{f})I_\mathrm{p}}{DE_\mathrm{s}} \qquad \text{(Eq. 2.5)}$$

where I_p is the displacement influence coefficient, and E_s is the elastic modulus of the soil.

The value of I_p is a function of the embedment ratio and foundation stiffness, obtained from the elastic solution by Mattes and Poulos [38]. The stiffness E_s is dependent on the stress state of the soil and the soil parameters that govern the modulus, which is nonlinear and stress-dependent. For spread foundations, the foundation and the soil immediately above the foundation are treated as a single block; thus, in Equation 2.5, W_f is replaced by the total weight of the foundation and soil immediately above the foundation ($W_\mathrm{f} + W_\mathrm{s}$) for spread foundations.

Table 2.2 Summary of failure criteria used for the interpretation of uplift loads (Adapted from Tang and Phoon [29], and Chen et al. [39]).

Basis of definition	Method/References	Interpreted capacity $Q_{u,int}$
Graphical construction	Tangent Intersection [40]	• Load at the intersection of two tangents to the initial and final linear sections of the Q-δ curve
	Slope Tangent [41]	• Load at a displacement equal to the initial slope of the Q-δ curve plus 0.15 in. (3.8mm)
	L_1-L_2 [36]	• Load L_1 and L_2 at the elastic limit and failure threshold, respectively.
	De Beer [42]	• Load at change in slope on log-log total settlement curve
	Fuller and Hoy [43]	• Minimum load that occurs for a rate of total settlement of 0.05 in per ton (0.14mm/kN)
Absolute movement limitation	Hansen [44] – 80% Criterion	• Load that gives four times the total movement as the movement obtained for 80% of that load
	Hansen [45] – 90% Criterion	• Load that gives twice the total movement as obtained for 90% of that load
Mathematical model	van der Veen [46]	• Load that gives a straight line when $\log(1-Q/Q_{u,int})$ is plotted
	Chin [47]	• Load equal to the inverse slope ($1/c_1$) of line $\delta/Q = c_1\delta+c_2$

Mattes Poulos [48] has verified the model with experiments on deeply embedded piles (avg. D/B = 15) with or without an enlarged base; however, the model was not evaluated with test results from shallow foundations. Moreover, since this model is based on elastic theory, the main obstacle to using this model is an accurate determination of the elastic modulus E_s of the soil [48] and the stiffness of the combined foundation and soil block. In general, it is difficult to predict the foundation displacements accurately, as the available models do not account for various influencing factors, including the soil behaviour and soil-foundation interaction characteristics [49].

2.2.2.2 Serviceability Requirements for the Uplift of Spread Foundations

In the SLS design, the foundation displacements are limited to satisfy the serviceability requirements, which are controlled by the limit state criteria of the supported structure. The allowable displacement level should be selected during the design process, with consideration that excessive foundation settlements or deformations can lead to failure in the supported structure [50].

The uplift displacements and limiting criteria of foundations have not been addressed in most design standards, including Eurocode 7 [3], the ASCE design standards for transmission tower structures [51], and the National Electrical Safety Code (NESC) [52]. However, the uplift displacement of individual foundations is a significant consideration for design conditions, where the uplift displacements lead to differential settlements of the foundations which can result in excessive stresses and potentially failure in the supported structure [4], [6], [7]. For transmission towers supported by four foundations, studies by the Electric Power Research Institute (EPRI) [4], [21] suggested the limiting uplift displacement of 25mm (1 in.), as structural instabilities were shown to develop at this value. This was based on the analytical results of the nonlinear structural model, where the uplift displacements of a single tower leg were increased, and the internal forces of the tower members were assessed at each displacement level (Figure 2.3).

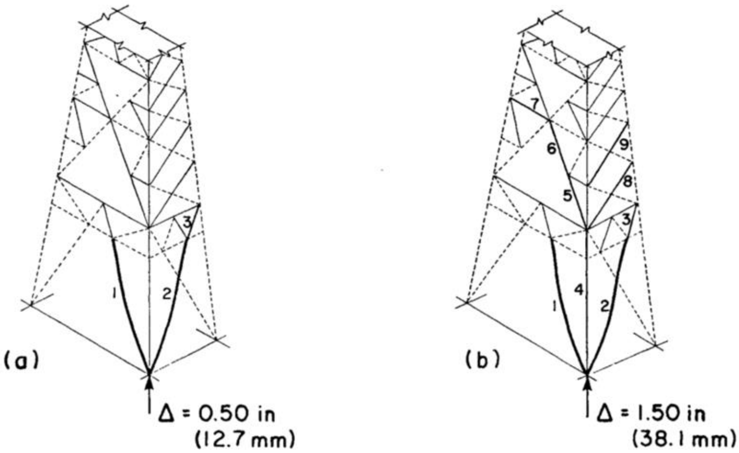

Figure 2.3 Force levels in the structural members of a transmission tower structure, caused by the uplift displacement of a single tower leg: (a) 0.50 in. (12.7mm) displacement; (2) 1.50 in. (38.1mm) displacement (Source: EPRI EL-2870 report [4]).

Since the focus of the SLS failure criteria is mainly placed on the differential settlement, the SLS criteria are usually suggested in terms of the differential vertical displacement or rotational displacement. For general structures, Eurocode 7 [3] states that the maximum relative rotational displacement of 1/500 is acceptable for many cases. The BS IEC 60826-2017 [53] design standard has suggested specific criteria for uplift displacements of transmission tower foundations, which are shown in Table 2.3.

2.3. Reliability-Based Design (RBD)

The design of geotechnical structures, including foundations, always involves uncertainties which arise from two main sources: (1) the variation in the soil properties and applied loads, and; (2) the calculation models that are used to estimate the foundation capacity or displacement (i.e. model uncertainty) [34], [54]. In addition to these sources of uncertainties, other factors such as the errors in the design and construction procedures may also affect the reliability of the foundation performance [55].

Conventionally, the uncertainties were dealt via the allowable stress design (ASD) approach, where a global factor of safety is applied. While the ASD approach has been widely used in practice, it was shown to have limitations in addressing the design uncertainties in a consistent manner [56]. As the values of the factors of safety are subjective and based on experience [57], [58], there are difficulties in yielding a consistent safety margin (i.e. reliability) against failure.

To overcome the limitations of the ASD approach, significant developments have been made in the reliability-based design (RBD) methods in the past decades. RBD is based on the principles of reliability analysis, where the uncertainties in the design and performance of the structure under consideration are evaluated in a quantitative manner [55]. This method was shown to give a more consistent level of reliability and the associated probability of failure, compared to the conventional ASD approach [59]. The key concepts of reliability analysis, and the reliability analysis methods that are used to develop RBD methods are detailed in the following subsections.

2.3.1 Performance Function and Probability of Failure

In reliability analysis, the probability of failure of the structure is assessed in terms of each limit state under consideration. The probability of failure (p_f) is defined as the probability of the applied loads Q exceeding the resistance of the structure R (Equation 2.6) [60].

$$p_{\mathrm{f}} = P(R - Q \leq 0) = P(g \leq 0) \qquad \text{(Eq. 2.6)}$$

where $P(\cdot)$ is the probability of occurrence, and g is the performance function.

The performance function, or limit state function, represents the margin of safety between the load and resistance ($g = R - Q$). The value of g is used to evaluate the failure state of the foundation; when $g < 0$, the structure is in failure condition, and when $g = 0$, the structure is at its limit state. Positive values of g (> 0) indicate a safe performance of the structure.

Table 2.3 Uplift displacement criteria for transmission tower foundations (Adapted from BS IEC 60826-2017 [53]).

Structure type	Statically determinate movement[1]	Displacement/Settlement criteria	
		Damage limit (SLS)	Failure limit (ULS)
Guyed[2]	Yes	Need to readjust tension in guys	Excessive out of plane movement (plane formed by the other three foundations) in the order of 50 – 100mm
	No	5% reduction in support strength	
Self-supporting[3]	Yes	1° (degree) rotation of the support	
	No	Differential vertical displacement of $Y/300 - Y/500$ (Maximum 20mm), where Y is the horizontal distance between foundations	

[1] Statically determinate movement is one that does not induce internal efforts in the structure (e.g. displacement of one foundation of a three-legged support is statically determinate, while displacement of four-legged support is statically indeterminate).

[2] Structure that is tied down by a set of guy wires and ground anchors for support.

[3] Structures that do not require external support (e.g. four-legged transmission tower).

Figure 2.4 illustrates the definition of the probability of failure p_f for random independent variables, R and Q. The definition of the reliability index β is also shown in the figure. The reliability index β can be computed with p_f via the following function (Equation 2.7) [61]:

$$\beta = -\Phi^{-1}(p_f) = \Phi^{-1}(-p_f) \quad \text{(Eq. 2.7)}$$

where $\Phi(\cdot)$ is a standardised normal distribution function.

To estimate the p_f and the related reliability β of the design through reliability analysis, the probability distribution characteristics of the applied load Q and resistance of the structure R need to be defined (incl. distribution type, mean, standard deviation, etc.). The characteristics are obtained by fitting a suitable distribution to the histogram of the obtained data for the load and resistance.

2.3.2 Reliability Analysis Methods for the Calibration of the Resistance Factor

The main objective of RBD is to ensure that the structure satisfies the targeted level of reliability and the probability of failure against each limit state for design. Specifically in the load and resistance factor design (LRFD) format, the load factors γ and the resistance factor ψ are applied to the applied loads and the resistance of the structure, respectively (Equation 2.1), in order to achieve the target reliability index β_T. The target reliability index is selected by considering various parameters, such as the reliability levels that are implicit in current design practice, and the failure consequences of the structure [23], [62].

For each load component Q_i, the load factor γ_i is estimated by assessing the statistics of the load data that is applicable to the type of structure and design model [63]. The load factors are usually selected from the values that are suggested in the existing RBD codes, such as AASHTO LRFD Bridge Design Specifications [1], based on the design loading case and load combination.

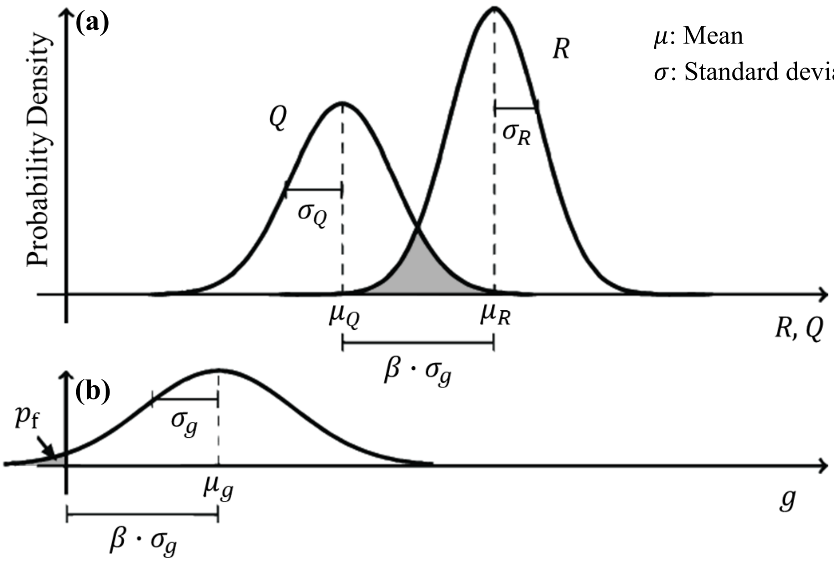

Figure 2.4 Definition of the probability of failure p_f and reliability index β for normal random variables, Q and R: (a) Joint distribution of Q and R; (b) Distribution of performance function g. The shaded area represents the failure probability p_f (Modified from Stipanovic et al. [64]).

The resistance factor ψ is calibrated via reliability analysis methods, with the following inputs: the selected load factors, and the probability characteristics of the load components and the resistance. The probability characteristics include the bias (λ), defined as the mean of the ratio between the measured and predicted value, and the coefficient of variation (COV), which is the ratio of the standard deviation to the mean of the distribution. Such probability characteristics represent the uncertainties in the estimated load and resistance of the structure, and are specifically referred to as "model statistics" for the resistance [29], [34], [54]. The model statistics are quantified via statistical analysis of geotechnical databases of load test results, and the associated properties of the foundation and soil. The types of reliability analysis methods that were commonly adopted in past studies are detailed as follows.

2.3.2.1 Approximate Reliability Analysis Methods

(1) *First Order Second Moment (FOSM)*

Based on the First Order Second Moment (FOSM) principles, simplified closed-form solutions have been suggested for the estimation of the resistance factors. The FOSM method assumes a normal or lognormal distribution for the variables of the performance function (i.e. R and Q), which allow for direct computations of ψ with the mean and COV of the variables only. The closed-form solution is expressed in Equation (2.8) [65]. As an example, the equation was provided for the case where only the dead and live loads are considered.

$$\psi = \frac{\lambda_{\mathrm{R}}\left(\gamma_{\mathrm{DL}}\frac{Q_{\mathrm{DL}}}{Q_{\mathrm{LL}}}+\gamma_{\mathrm{LL}}\right)\sqrt{\frac{1+\mathrm{COV}_{\mathrm{DL}}^2+\mathrm{COV}_{\mathrm{LL}}^2}{1+\mathrm{COV}_{\mathrm{R}}^2}}}{\left(\lambda_{\mathrm{D}}\frac{Q_{\mathrm{DL}}}{Q_{\mathrm{LL}}}+\lambda_{\mathrm{LL}}\right)\exp\left\{\beta_T\sqrt{\ln\left[(1+\mathrm{COV}_R^2)(1+\mathrm{COV}_{DL}^2+\mathrm{COV}_{LL}^2)\right]}\right\}} \qquad \text{(Eq. 2.8)}$$

where the subscripts R, DL, and LL denote the resistance, dead loads, and live loads, respectively. The variables are expressed as lognormal random variables.

Despite the simplicity of the FOSM method, the simplification and linearisation of the solution may lead to errors in the results for cases that involve highly nonlinear problems, which may include correlated variables or variables with different probability distributions (e.g. Gumbel, Weibull, exponential, etc.) [61], [66], [67]. In addition, the method fails to be invariant to different equivalent formulations of the performance function [68], which means that the closed-form solutions and the analysis results are dependent on the way the performance function is formulated.

(2) *First Order Reliability Method (FORM)*

First Order Reliability Method (FORM) is an approximate method, which has been widely applied for structural reliability analyses [69]. The method was originally developed by Hasofer and Lind [70] as an invariant method for estimating the reliability of the structure. The FORM involves a linear approximation of the limit state function, which is often nonlinear, to identify the most probable point (MPP) of failure. The limit state is linearised at the MPP, which is adjusted via an iterative procedure to estimate the minimum value of the reliability index β (i.e. highest p_f). The accuracy of the results from FORM is dependent on the extent of the nonlinearity of the limit state function [71], [72]. For linear limit state functions, FORM gives an exact solution, while the accuracy of the method may decrease for functions with a strong non-linearity and a large number of random variables [73].

2.3.2.2 Monte-Carlo Simulation (MCS)

Monte-Carlo Simulation (MCS) is a practical method that can be applied to variables with any type of probability distribution and correlation structures. In the MCS method, a large number of samples of the variables in the performance function g are generated, based on the defined probability distribution characteristics of each variable. With the generated samples, the probability of failure is directly calculated as follows (Equation 2.9) [26].

$$p_{\mathrm{f}} = \frac{1}{N_{\mathrm{s}}} \sum_{i=1}^{N_s} I[g_i \leq 0] \qquad \text{(Eq. 2.9)}$$

where N_s is the number of simulations, I is the indicator function which is equal to 1 when $g_i \leq 0$ (i.e. failure state), and 0 when $g_i > 0$ (i.e. safe state).

Equation 2.9 is essentially the ratio between the number of failure cases (i.e. sum of the indicator function) and the total number of simulations. While keeping the load factors constant, the value of the resistance factor ψ is adjusted until the target probability of failure, or reliability level, is achieved. Generally, the results from MCS method are taken as "exact" or "accurate", as this method is shown to yield more accurate results, compared to the other approximate or iterative reliability analysis methods (e.g. FOSM and FORM) [26], [74]. Due to its versatility and accuracy, the MCS method has been adopted in numerous recent studies for the reliability analysis of structures including foundations [18]–[20], [75].

2.4. Development Frameworks for RBSLS Design Methods

The reliability-based serviceability limit state (RBSLS) design method assesses whether the foundation fulfils the SLS criteria with the targeted level of reliability. In terms of the SLS, the structure fails when the displacement of the structure exceeds the allowable displacement level. Overall, previous studies have developed two main frameworks and approaches for the development of RBSLS design methods: the displacement-based approach, and the empirical model approach.

2.4.1 Displacement Model Factor Approach

The uncertainties in the displacement can be quantified through the statistical characterisation of the displacement model statistics. The displacement model statistics are represented by the probability distribution characteristics of the displacement model factor, or settlement ratio (SR), which is defined as follows [12], [13], [29].

$$SR = \frac{\delta_{\text{measured}}}{\delta_{\text{calculated}}} \quad \text{(Eq. 2.10)}$$

where δ_{measured} and $\delta_{\text{calculated}}$ are the measured and calculated displacements, respectively.

The value of the calculated displacement $\delta_{\text{calculated}}$ at a given load is computed from relevant prediction models. In this case, the performance function is expressed as $g = \delta - \delta_{\text{all}}$ or $g = \delta/\delta_{\text{all}}$ for the movement mode of interest (e.g. immediate settlement, lateral or uplift movement of the foundation). This approach was utilised in several research programs, including National Cooperative Highway Research Program (NCHRP) [23], SHRP2 [14], and the subsequent studies by the Federal Highway Administration (FHWA) [12], [13], all of which were carried out to implement RBSLS design methods into the AASHTO design code for bridge foundations.

While this approach is consistent with the method for evaluating the ULS capacity model statistics, it cannot be applied to design conditions with no available prediction models for the computation of $\delta_{\text{calculated}}$. In addition, this method does not capture the whole load-displacement relation of the foundation, which implies that the analysis procedures would need to be repeated if a different SLS criterion was to be considered.

2.4.2 Empirical Model Approach

The limitations of the displacement-based approach can be overcome by adopting the empirical model approach, where the load-displacement relation of the structure is modelled as an empirical function. For this approach, calculation models for the displacement prediction are not required, as the uncertainties in the load at a given displacement, and vice versa, can be obtained from the statistics of the model parameters that characterise the load-displacement curves. The performance function is expressed in terms of the loads, as shown in Equation 2.11. To capture the nonlinearity of the relation, bi-variate nonlinear models such as the power law model or hyperbolic model are usually used.

$$g = Q - Q_{\text{all}} = Q - Q_{\text{u}} M_{\text{SLS}}(\delta_{\text{all}}) \qquad \text{(Eq. 2.11)}$$

where Q_{all} is the allowable load that corresponds to the allowable displacement level, and M_{SLS} is the SLS model factor that represents the empirical model which is a function of the allowable displacement.

Over the past several decades, significant advances have been made to optimise and improve the accuracy of the outputs from this approach. Some early studies have been conducted in the EPRI TR-105000 report [21], where bi-variate hyperbolic and power law models were adopted to calibrate the SLS resistance factors for δ_{all} = 25mm, 38mm, and 50mm (1 in, 1.5 in, 2 in). An example of the modelled load-displacement curves is shown in Figure 2.5. However, the study by the TR-105000 report [21] did not consider several considerations, such as the correlation between the parameters. The correlation and statistically significant dependencies between the variables need to be checked, in order to be consistent with the assumptions of reliability analyses that the variables are independent and random [51], [76].

Phoon et al. [76] assessed the load-displacement curves of spread foundations and drilled shafts to check for any correlation between the model parameters. The findings demonstrated that a statistically significant negative correlation was present between the model parameters, suggesting that it is not justifiable to treat the parameters as random variables. The same observations have been made from most other studies that used the empirical model approach for the development of RBSLS design methods [15], [51].

The correlation can be characterised via various correlation coefficients and models. Phoon et al. [76], Phoon and Kulhawy [15], and Dithinde et al. [51] used an equivalent normal correlation coefficient (Pearson correlation coefficient ρ) for the model parameters with lognormal distributions. However, the use of this correlation coefficient is based on the assumption that the variables are linearly correlated, which may not be applicable to nonlinear correlation structures. To develop appropriate models for nonlinear correlation structures, several studies have implemented the use of copula analysis and models in the RBSLS procedures [16]–[19], [77], [78]. Copula functions express the multivariate joint distribution functions with their one-dimensional marginal distributions [79]. The functions are dependent on the copula parameters and the Kendall's tau correlation coefficient ρ_τ which represent the strength of the correlation.

While various studies have been carried out on the implementation of the correlation between the model parameters, there have been limited studies that involve the treatment of statistically significant dependencies between the model parameters and foundation parameters. While such dependencies were not assessed or observed in most studies, Stuedlein and Reddy [80] reported that strong dependencies were present between the model parameters and the pile slenderness (i.e. ratio of pile length to diameter *D/B*) for augered cast-in-piles in cohesionless soils. The dependencies were treated by dividing the model parameters by *D/B* or $(D/B)^{-0.5}$, although no specific reason was provided for the choice of the exponents.

In addition, no studies to date have explicitly addressed the errors that arise from the deviation between the measured curves and the fitted empirical models. The errors have been used to compare the accuracy of different empirical models, but with no further considerations in the estimation of the foundation reliability. Although fitting errors are evident and inevitable, such errors are yet to be incorporated into the RBSLS development procedures.

Furthermore, the current RBSLS procedures do not account for the relationship between the SLS and the ULS. It has been shown by Wang [22] and Orr [9] that the SLS governs the design of foundations with large widths and load capacities, and low allowable displacement values (i.e. SLS criteria) [9], [22]. For opposite conditions, the ULS governs the design and the SLS requirements are automatically satisfied. While the governing limit state may affect the foundation design, and the associated reliability of the foundation for each limit state, such considerations have not been implemented in the current RBSLS design methods.

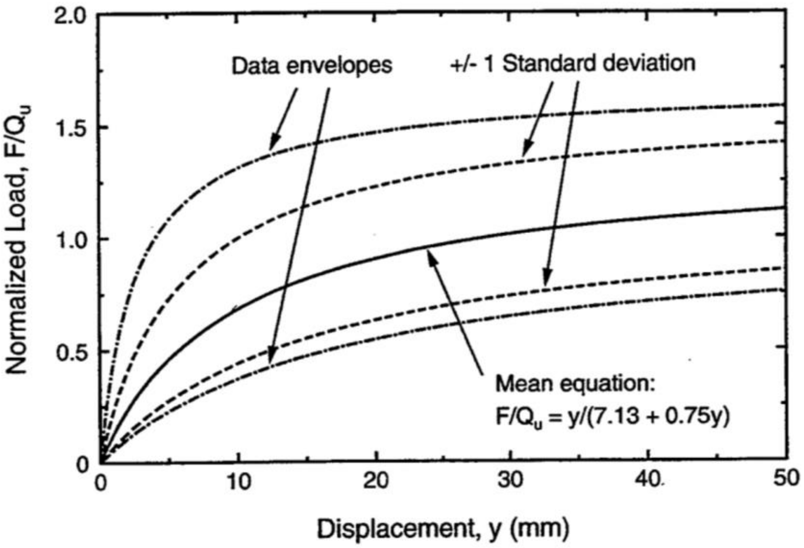

Figure 2.5 Load-displacement curves of spread foundations under uplift loading (Hyperbolic model; Source: TR-105000 report [21]).

2.5. Summary

The literature review focussed on the limit state design of spread foundations under uplift loading in cohesionless soils, specifically on the reliability-based serviceability limit state design. The following subjects have been discussed: (1) the main limit states for design, including the ULS and SLS, along with the available calculation models for the prediction of the capacity and displacement; (2) definition and criteria for the failure condition in terms of each limit state; (3) the concepts of reliability-based design methods and the reliability analysis procedures, and; (4) the existing frameworks for the development of RBSLS design methods.

Outstanding issues have been identified from the literature review, which could be addressed in the development of the RBSLS design procedures for spread foundations subjected uplift loads in cohesionless soils:

1. Currently, there are no available calculation models specifically for the prediction of the uplift displacement of spread foundations. Consequently, there are no SLS design methods that are used in practice for this specific design condition. Thus, to allow for the development of RBSLS design methods for this condition, an empirical characterisation would be required

for the probabilistic analysis of the load-displacement behaviour of the foundation.

2. Up to date, various studies have been conducted to improve the RBSLS design procedures for its implementation in practice. However, the suggested frameworks for the RBSLS design procedures do not include some statistical considerations. This includes the assessment and treatment of the statistical dependencies between the empirical model parameters and the foundation design parameters, and the errors between the measured load-displacement curves and the fitted curves from the empirical model. Thus, to ensure the randomness of the parameters and to improve the accuracy of the reliability analysis outcomes, it would be necessary to incorporate the above-mentioned factors into the RBSLS development procedures.
3. Current research on the reliability-based design and limit state design methods do not consider the relationship between the two main limit states (i.e. ULS and SLS), as they focus separately on the individual limit states. Thus, it is seen that additional work is required to analyse the effects of the relationship between the limit states, such as the governing limit state, on the RBSLS design procedures of the foundation.

Chapter 3. Characterisation of the Uplift Load-Displacement Curves

3.1. Compilation of Load Test Database

A database of 61 load test data from spread foundations under uplift loading in cohesionless soils was compiled for this study. The summary of the database is provided in Table 3.1. The database consists of the load-displacement curves and the associated properties of the soil and foundation, which were obtained from four different sources that investigate the uplift behaviour of spread foundations [81]–[84]. The types of spread foundations in the database include plate anchors, footings, and belled piers. The sources were selected, mainly by referring to the sources in the NUS/SpreadFound/919 database by Tang et al. [20] which also covers the foundation type and design condition of interest for this study. The detailed database is included in Appendix A.

When compiling the database, the following criteria were considered: (1) sufficient description of the load test conditions and soil properties; (2) cohesionless soils above the foundation base that is relatively dry and uniform; (3) uniaxial uplift loading conditions without any loading and unloading cycles, or inclination in the applied loads; (4) foundation widths (B) greater than 0.30m, so that the data is representative of the behaviour of full-scale foundations, and; (5) shallow foundations with the embedment ratio (D/B), defined as the ratio of the embedment depth to the foundation width, of less than 6. The last criterion was considered to minimise the scatter in the compiled data, since the load-displacement behaviour of shallow foundations can significantly differ from that of deeply embedded foundations [85], [86]. Among the compiled load-displacement curves, some of the curves showed a distinct peak in the load, followed by a softening behaviour with a significant decrease in the load. In this case, the peak load was taken as the ultimate capacity (Q_u) of the foundation, and the portion of the curves at further displacements after the peak load was neglected.

The sample size of N=61 was seen to be sufficient, as it lies within the range of the sample size that was considered in past literature. Various studies on the

RBSLS of spread foundations adopted the sample size of N=30 [16], [17], [78], [87]. A larger sample size was considered in the studies by Stuedlein and Uzielli [19] for helical anchors in clay under uplift loading (N=37), and Tang et al. [20] for spread foundations in cohesive (N=44) and cohesionless soils (N=67) under uplift loading. Thus, the sample size of $N \geq 30$ is seen to be generally acceptable, particularly since there is a relatively small database for uplift load tests, compared to compression load tests. As an additional analysis, a convergence test was carried out in Appendix B, based on the results that were obtained from the subsequent sections (Sections 3.2-3.5).

Table 3.1 Summary of the load test database for spread foundations under uplift loading in cohesionless soils.

Foundation Type	Test Type	Soil Type	Number of data N	Foundation Shape and Width B (m)	Embedment Ratio D/B	Friction Angle ϕ (°)	Reference
Plate Anchor	Field	Alluvial fine-grained sand	5	Circular: 0.40 – 1.20	0.8 – 2.5	32	Kananyan [81]
		Non-plastic, uniform fine sand	3	Circular: 0.30	1.0 – 2.0	39	Consoli, Ruver, and Schnaid [82]
Footing	Centri-fuge	Fine silica sand	12	Square: 3.50 – 6.50	0.7 – 1.4	37 – 43	Gu et al. [83]
Belled Pier	Field	Gobi gravel (well-graded gravel with cobbles)	41	Circular: 1.01 – 2.29	1.5 – 3.5	42	Qian et al. [84]
All			61	0.30 – 6.50	0.7 – 3.5	32 – 43	

3.2. RBSLS Procedures and Limit State Models

For the RBSLS, it is critical to incorporate all sources of uncertainties that affect the load-displacement behaviour and the reliability of the foundation. The reliability of the foundation is related to the probability of failure, where the foundation displacement (δ) exceeds the allowable displacement (δ_{all}). The failure can be written in terms of the loads, where the applied loads exceed the allowable load (Q_{all}) that corresponds to δ_{all} at the load-displacement curve of the foundation (Equation 3.1).

$$p_{\mathrm{f}} = P(\delta_{\mathrm{all}} < \delta) = P(Q_{\mathrm{all}} < Q_{\mathrm{app}}) \quad \text{(Eq. 3.1)}$$

where Q_{app} is the uplift loads applied to the foundation.

The uncertainties in the foundation displacement δ under the applied loads can be estimated from the scatter in the load-displacement curves of the foundation. For this study, the uncertainties in the curves were characterised, mainly by using the procedures of the general framework by Huffman et al. [17]. While the framework was developed for the RBSLS design of aggregate pier-reinforced grounds, the main considerations and procedures of the framework were adopted. One of the key procedures is the transformation of the ULS-based capacity (Q_{u}) to the load-displacement relation of the foundation, where the displacement is expressed in terms of the mobilised loads, relative to Q_{u}. This requires both the ultimate and serviceability limit state models which define the predicted ultimate capacity and the load-displacement relation of the foundation, respectively.

Two main types of SLS models exist for representing the nonlinear load-displacement relationship of the foundation: the hyperbolic model, and the power law model [19], [78], [87]. The model is fitted to the normalised curves, where the mobilised loads are normalised by the reference capacity (Q_{ref}), and the displacement by the equivalent foundation width (B'). For square foundations, the equivalent width is the diameter of a circular foundation that gives the same base area [88]. The function of the hyperbolic model is written as

$$\frac{Q}{Q_{\mathrm{ref}}} = \frac{\eta}{\theta_1 + \theta_2 \eta} \quad \text{(Eq. 3.2)}$$

where η is the pseudo-strain ($=\delta/B'$), and θ_1 and θ_2 are best-fit empirical fitting coefficients of the hyperbolic model. It is to be noted that each fitting coefficient has a physical meaning, where θ_1 corresponds to the reciprocal of the initial slope, and θ_2 to the reciprocal of the final asymptote of the hyperbolic curve. The power law model is expressed as

$$\frac{Q}{Q_{\mathrm{ref}}} = \theta_3 \eta^{\theta_4} \quad \text{(Eq. 3.3)}$$

where θ_3 and θ_4 are best-fit empirical fitting coefficients of the power law model.

The SLS models can be associated with the ULS-based capacity of the foundation via the model factor, which is defined as the following ratio:

$$M_{\mathrm{ULS}} = \frac{Q_{\mathrm{ref}}}{Q_{\mathrm{uc}}} \tag{Eq. 3.4}$$

where M_{ULS} is the capacity model factor, and Q_{uc} is the predicted ultimate capacity of the foundation that is computable with the existing calculation models (i.e. ULS models).

The ULS models for the uplift capacity prediction are well-documented in several guidelines for the design of transmission tower foundations. This includes the IEEE guide [5] and the DS-1110 standards from the Korea Electric Power Corporation [89]. Among the different available models, the Meyerhof and Adams [28] method was selected as the ULS model for this study. This method is a general semi-empirical method that has been evaluated in past studies about the reliability of foundations under uplift forces [29], [90]. The method is applicable to a wide range of design conditions, as it considers the effects of various design parameters on the uplift failure mechanism and ultimate capacity of the foundation. By incorporating M_{ULS}, an estimation of Q_{ref} can be made from the calculated capacity Q_{uc} with some degree of uncertainty that is represented by the statistics of M_{ULS} (i.e. capacity model statistics). This allows for the transformation of the calculated ULS capacity Q_{uc} to the normalised load-displacement curves, expressed in terms of Q_{ref}.

3.3. Normalisation of the Load-Displacement Curves

For the normalisation of the load-displacement curves, different normalisation protocols were compared to identify the optimal option that gives the least scatter in the normalised curves. In this study, the considered reference capacities for the normalisation of the loads are the tangent intersection capacity (Q_{TIU}), and the slope tangent capacity with the offset of $0.01B$ ($Q_{0.01\mathrm{B}}$) and $0.02B$ ($Q_{0.02\mathrm{B}}$). The definitions of the reference capacities are illustrated in Figure 3.1. The tangent intersection capacity is the load at the intersection between the tangent lines of the initial and final linear sections of the load-displacement curve. The capacity Q_{TIU} was considered, as it was interpreted as the ultimate uplift capacity for spread foundations by Kulhawy et al. [4]. The slope tangent capacity is the load, where the initial tangent line with the specified displacement offset intersects the load-displacement curve. The slope tangent capacities, with arbitrary offset values of (0.01~0.1)B, have been widely adopted in various studies for the RBSLS of foundations [15], [17]–[19]. For this study, the offset values of 0.01B and 0.02B were used, as there are fewer data that reach larger displacements.

Figure 3.2 compares the load-displacement curves that were normalised with different normalisation protocols. In general, the normalised curves display a clear hyperbolic trend with a significant reduction in scatter. It was shown that each normalisation protocol resulted in different levels of scatter that varied depending on the displacement level. The normalisation by Q_{TIU} (Figure 3.2b) gave a consistent level of scatter throughout the whole range of displacement, with some of the curves deviating from the overall hyperbolic trend. For the normalisation by $Q_{0.01\mathrm{B}}$ or $Q_{0.02\mathrm{B}}$ (Figures 3.2c-d), the curves tended to merge towards the point, where (Q/Q_{ref}) is equal to unity. The merging occurred at higher displacements with an increase in the displacement offset from 0.01B to 0.02B. This resulted in the curves normalised by $Q_{0.01\mathrm{B}}$ to show improved scatter at lower displacements, while normalisation by $Q_{0.02\mathrm{B}}$ showed improved scatter at further displacements.

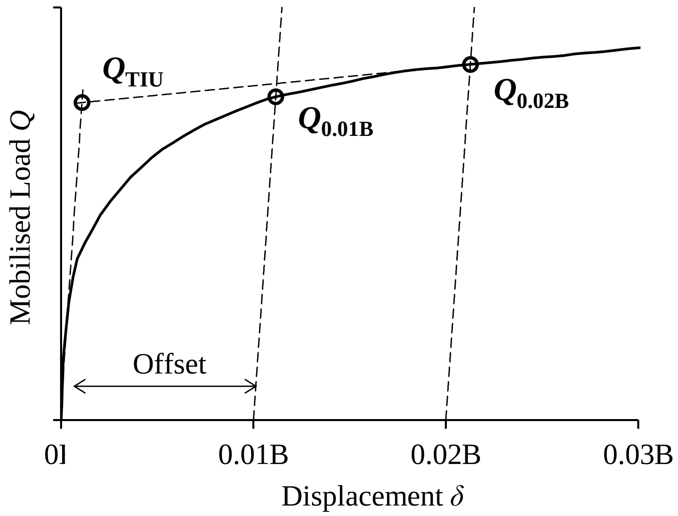

Figure 3.1 Definition of the tangent intersection uplift capacity (Q_{TIU}) and slope tangent capacities with the offset of 0.01B ($Q_{0.01\mathrm{B}}$) and 0.02B ($Q_{0.02\mathrm{B}}$).

From visual inspection, it is unclear which normalisation protocol gives the least scatter in the normalised curves. Thus, further analyses were carried out to evaluate and compare the scatter in the normalised curves.

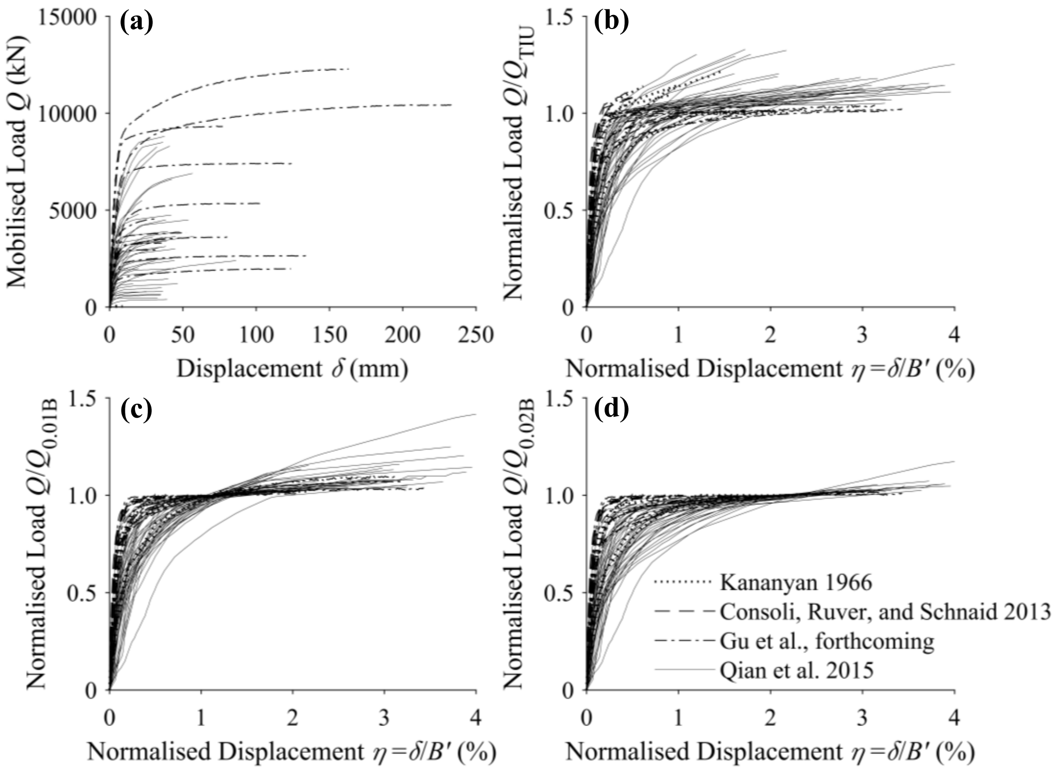

Figure 3.2 Comparison of the raw and normalised load-displacement curves of spread foundations in cohesionless soils under uplift loading: (a) raw curves; (b) load normalised with the tangent intersection capacity; (c) load normalised with the slope tangent capacity with 0.01B offset; (d) load normalised with the slope tangent capacity with 0.02B offset

3.4. Selection of the SLS Model and the Evaluation of the Fitting Errors

The uncertainties in the normalised load-displacement curves can be represented by the scatter in the empirical fitting coefficients, which are obtained by fitting the SLS models to the curves. For the fitting process, the least-squares method was applied by using the Curve Fitting Toolbox in MATLAB R2021a [91]. Among the power law and hyperbolic models, a suitable SLS model was selected by evaluating the goodness of fit of each model and the fitting errors between the measured and fitted curves. The goodness of fit was evaluated with the root mean squared error (RMSE), which is a statistical measure that is appropriate for both linear and nonlinear models [92]. The equation for the RMSE is shown below in Equation 3.5.

$$RMSE = \sqrt{\frac{\sum_{i=1}^{N}|y_i - \hat{y}_i|^2}{N}} \qquad \text{(Eq. 3.5)}$$

where y_i is the measured value, $\hat{y}_i$ is the corresponding prediction value from the empirical model, and N is the number of data points.

Table 3.2 presents the values of the RMSE and the proportion of the RMSE, relative to the maximum value of the normalised load (Q_{max}/Q_{ref}). It was shown that the RMSE values and the RMSE relative to (Q_{max}/Q_{ref}) are significantly lower for the hyperbolic model, compared to the power law model. The relative RMSE was identical for all normalisation protocols, with an average value of 3.30% for the hyperbolic model and 8.62% for the power law model. This indicates that the hyperbolic model provided a better fit than the power model.

In addition, the fitting errors that arise from the fitting process were assessed. Although there are evident differences between the measured and fitted curves, such errors have not been explicitly addressed in past literature. It was attempted in this study to quantify the fitting errors with the ratio of the measured load to the predicted load from the fitted curves at each displacement level, which is referred to as the fitting model factor in this study ($M_{fit}=Q_{measured}/Q_{fitted}$). Figure 3.3 shows the variation in the fitting model factor M_{fit} over displacement for each load-displacement curve. Overall, it was found that M_{fit} is independent of the normalisation protocol. Both models display significant fitting errors at low displacement levels, as indicated by the M_{fit} values that lie outside the range of 0.5–1.5 (i.e. ±50% difference in the load between the measured and fitted curves). This can be explained by the fact that the values of the loads are small at the initial portion of the curves, which causes the difference between the measured and fitted curves to yield a larger percentage error, and therefore values of M_{fit} that are further from unity. Compared to the power law model, the M_{fit} values from the hyperbolic model were generally closer to unity. Also, the scatter in M_{fit} at each displacement level was relatively small, particularly at large displacements, indicating that the measured and fitted curves are in good agreement.

Table 3.2 RMSE of the fitted hyperbolic and power law models.

SLS Model	Reference Capacity	Average (Range)	
		RMSE	RMSE/($Q_{\text{max}}/Q_{\text{ref}}$) (%)
Hyperbolic	Q_{TIU}	0.030 (0.010–0.089)	3.30 (0.84–7.41)
	$Q_{0.01\text{B}}$	0.035 (0.009–0.092)	
	$Q_{0.02\text{B}}$	0.034 (0.008–0.077)	
	All	0.035 (0.008–0.092)	
Power Law	Q_{TIU}	0.095 (0.037–0.132)	8.62 (2.61–13.05)
	$Q_{0.01\text{B}}$	0.091 (0.042–0.131)	
	$Q_{0.02\text{B}}$	0.087 (0.034–0.131)	
	All	0.091 (0.034–0.132)	

The statistics of M_{fit} were obtained at each displacement level (Figure 3.4), which can be incorporated as fitting uncertainties into the reliability analysis procedures. When obtaining the statistics of M_{fit}, a lognormal distribution was assumed, as it allows for non-negative values only for the model factor. As expected, the hyperbolic model gave the mean and the coefficient of variation (COV) of the M_{fit} that are closer to unity and zero, respectively, compared to the power law model; this is consistent with the observations made in Figure 3.3. Based on the findings from the statistical evaluation of the SLS models, the hyperbolic model was selected as the SLS model for the normalised curves.

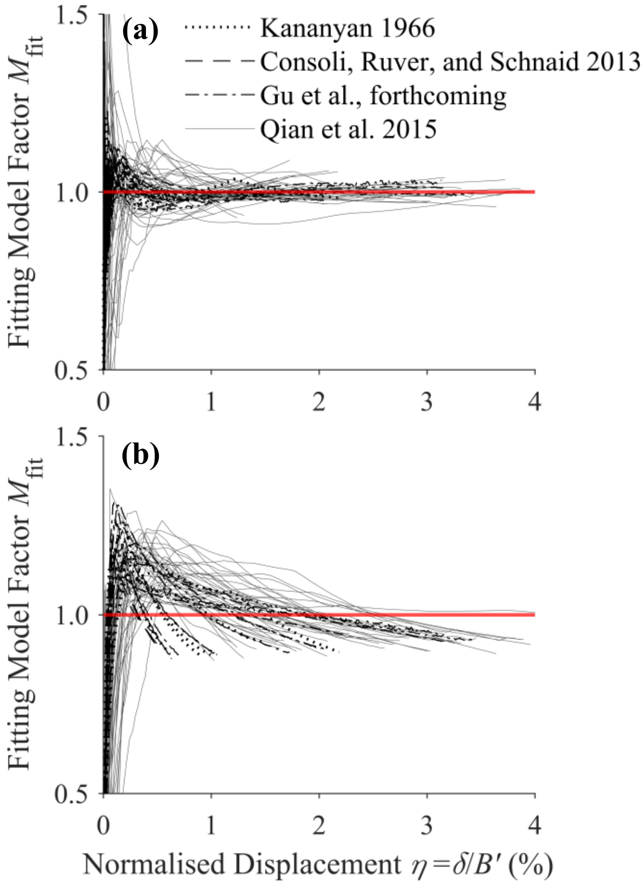

Figure 3.3 Variation in the fitting model factor M_{fit} over the normalised displacement η: (a) hyperbolic model; (b) power law model.

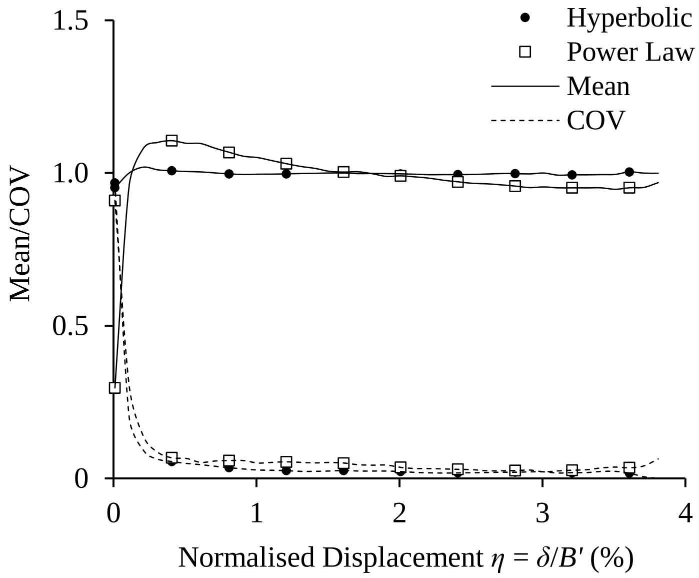

Figure 3.4 Variation in the mean and coefficient of variation (COV) of the fitting model factor M_{fit} over the normalised displacement η.

3.5. Selection of the Normalisation Protocol

The selection of the normalisation protocol requires the evaluation of the empirical fitting coefficients of the normalised curves, and the model uncertainties in the estimation of Q_{ref}. As these parameters directly affect the estimated reliability of the foundation, the variance in the fitting coefficients and the model uncertainties should be minimised for a more accurate assessment of the foundation reliability. With reference to the framework by Huffman et al. [17], the statistical characteristics of the coefficients and the capacity model uncertainties from each normalisation protocol were compared to support the decision-making process.

3.5.1 Evaluation of the Scatter in the Fitting Coefficients

Firstly, the values of the coefficients θ_1 and θ_2 were obtained by fitting the hyperbolic model to the normalised curves. The lognormal distribution and the generalised extreme value distribution were fitted to θ_1 and θ_2, respectively. The suitability of the functions was evaluated by using the Anderson-Darling test, which is a statistical test of assessing whether the input data samples are obtained from the selected distribution [93]. It was found that the p-values of the Anderson-Darling test were greater than 0.05, indicating that the fitted distributions are appropriate. Figure 3.5 shows the cumulative probability distributions of the fitting coefficients. The figure shows that the distributions of θ_1 were nearly identical for all normalisation protocols. On the other hand, the distributions of θ_2 from the normalisation by $Q_{0.01B}$ showed the smallest range of values, which indicates that the curves normalised by $Q_{0.01B}$ have the least scatter with the smallest range of possible displacements at a given load, and vice versa.

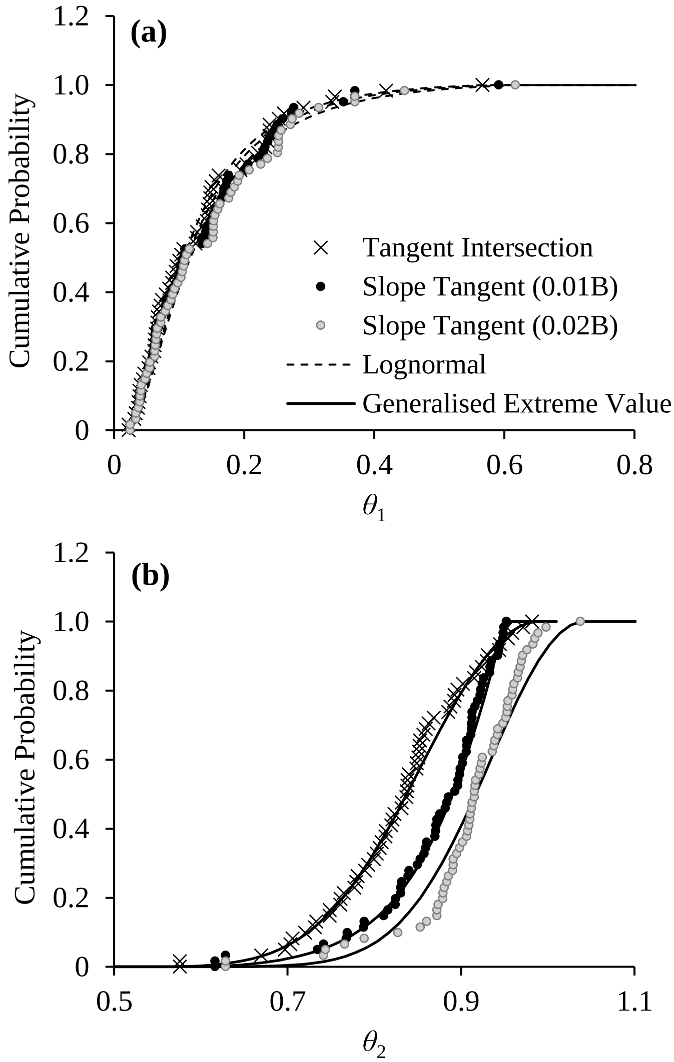

Figure 3.5 Sample and fitted cumulative probability distributions of the hyperbolic fitting coefficients from each normalisation protocol: (a) θ_1; (b) θ_2.

3.5.2 Evaluation of the Correlation Between the Fitting Coefficients

Secondly, the correlation between the fitting coefficients was assessed, as illustrated in Figure 3.6. The non-parametric Kendall's tau correlation coefficient (ρ_τ) was used to characterise the correlation, as it is relatively insensitive to discrepancies in the data, and is directly applicable to the use of copula theory. As shown in Figure 3.6, a negative correlation was observed between the fitting coefficients from all normalisation protocols. The magnitude of ρ_τ, and therefore the strength of the correlation, was significantly higher for the normalisation by $Q_{0.01B}$ ($|\rho_\tau|$=0.726), compared to the other two normalisation protocols ($|\rho_\tau|$=0.434–0.461). For negatively correlated coefficients of a bi-variate hyperbolic model, a stronger correlation indicates smaller scatter in the normalised load-displacement curves [15], which implies that the normalisation by $Q_{0.01B}$ yields smaller scatter in the curves.

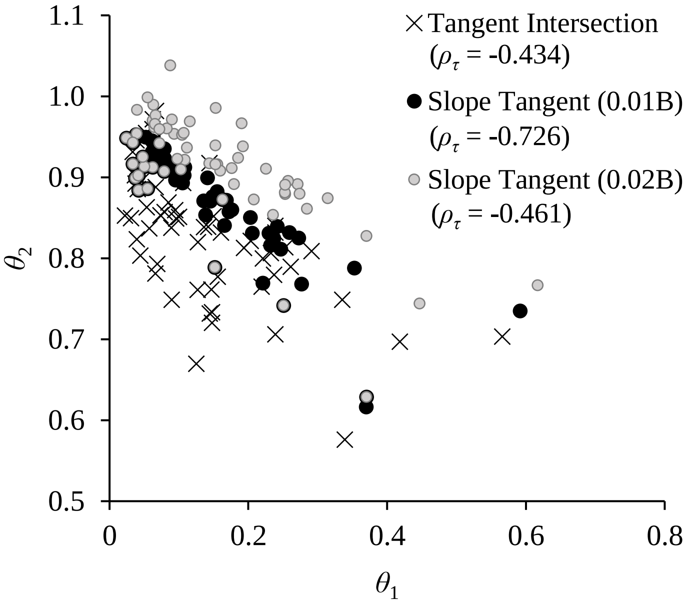

Figure 3.6 Correlation between the hyperbolic fitting coefficients from each normalisation protocol.

3.5.3 Evaluation of the Model Uncertainties

The reference capacities were compared with the predicted ultimate capacity Q_{uc}, computed with the ULS model of this study (Figure 3.7). The model uncertainty in Q_{ref} was evaluated with the capacity model statistics (i.e. mean and COV of M_{ULS}), which were obtained by assuming a lognormal distribution. The lognormal distribution was used to allow for positive values only, since model factors cannot be negative or zero [62], [94], [95]. Figure 3.7 shows that the model statistics of all reference capacities were generally similar, with the bias μ (i.e. mean of M_{ULS}) that ranges from 1.58 to 1.74, and the COV of 0.53 to 0.55. Thus, the model statistics do not provide significant decision-making support.

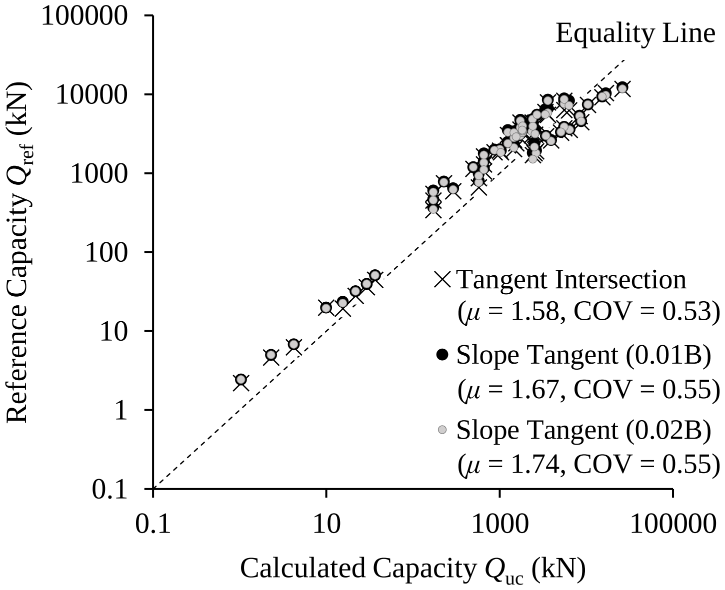

Figure 3.7 Comparison of the reference capacity (Q_{ref}) and the predicted ultimate capacity (Q_{uc}) calculated with the Meyerhof and Adams [28] method.

3.5.4 Selected Normalisation Protocol

For the selection of the normalisation protocol, the main objective should be to minimise the scatter in the fitting coefficients, as it is seen to have the highest influence on the overall uncertainties in the normalised curves [17]. With this consideration and the comparisons in Figure 3.5-3.7, it was deduced that the normalisation by $Q_{0.01B}$ is the optimal normalisation protocol. This protocol yielded the least scatter in the hyperbolic fitting coefficients, as demonstrated by the relatively small scatter in the probability distributions and the strong negative correlation between the coefficients (ρ_τ=-0.726). Also, the capacity model statistics (μ=1.67, COV=0.55) demonstrated that the $Q_{0.01B}$ could be estimated reasonably with the chosen ULS model. Thus, the fitting coefficients of the curves normalised by $Q_{0.01B}$ were used for further analyses of this study.

3.6. Statistical Assessment of the Fitting Coefficients

3.6.1 Statistical Dependencies on the Foundation Design Parameters

Since reliability-based analyses and design methods assume that the parameters are independent and random, it should be checked whether there are any statistically significant dependencies between the fitting coefficients and the design parameters of the foundation [15], [34]. The identified dependencies need to be removed via statistical procedures, such as regression analysis, in order to consider the parameters as random variables for the implementation of the RBD [20], [95]. The shape of the load-displacement curves, and therefore the model fitting coefficients, can be affected by various parameters of the foundation and soil. This includes the friction angle of the soil, and the embedment ratio of the foundation [86]. Potential dependencies on the foundation width were also assessed, as scale effects may be present [94], [96].

The relationship between the fitting coefficients and foundation design parameters is shown in Figure 3.8. The statistical significance was checked via the Spearman's correlation test, where the Spearman's p-value of less than 0.05 indicates a statistically significant relationship. The figure shows that θ_1 has a statistically significant dependency on all the parameters (p<0.05). For θ_2, the dependency is present for all parameters, except for the friction angle. The dependency of the coefficients on the embedment ratio D/B of the foundation is particularly strong, as shown by the low Spearman's p-values of 8.52×10^{-15} and 8.31×10^{-12} for θ_1 and θ_2, respectively. The low p-values indicate that there is a substantially lower probability of the statistically significant relationship occurring by chance [97], compared to the other two parameters. Thus, to remove the observed dependencies, the strongest dependency was treated first by performing regression analysis on coefficients θ_1 and θ_2 against D/B. With reference to Tang et al. [20], the following regression function was applied:

$$\theta_i = f_i \theta_{i,\mathrm{t}} = \left[a_i \left(\frac{D}{B} \right)^{b_i} \right] \theta_{i,\mathrm{t}} \qquad \text{(Eq. 3.6)}$$

where the subscript i=1, 2 corresponds to the respective fitting coefficients (θ_1, θ_2), f_i is the regression function used to remove the statistical dependency, a_i and b_i are the best fit coefficients of the regression function, and $\theta_{i,\mathrm{t}}$ is the treated fitting coefficient that is obtained from the removal of the statistical dependency. The regression functions are shown in Figure 3.8a which are applicable to the range of D/B=0.7–3.5.

The treated coefficients $\theta_{1,\mathrm{t}}$ and $\theta_{2,\mathrm{t}}$ showed no dependencies on all the considered parameters (p>0.05), as shown in Figure 3.9, meaning that the treatment of the dependencies on D/B removed the dependencies on all the other foundation design parameters. This may be due to the removal of the major trend in the fitting coefficients, which would have decreased the statistical significance of other dependencies, and the partial addressment of the foundation width by the D/B in the regression function. For the reliability analysis, the treated coefficients $\theta_{1,\mathrm{t}}$ and $\theta_{2,\mathrm{t}}$ were back-transformed to the coefficients θ_1 and θ_2 with the deterministic values of D/B=1, 2, 3, considering the applicable range of D/B of the regression function.

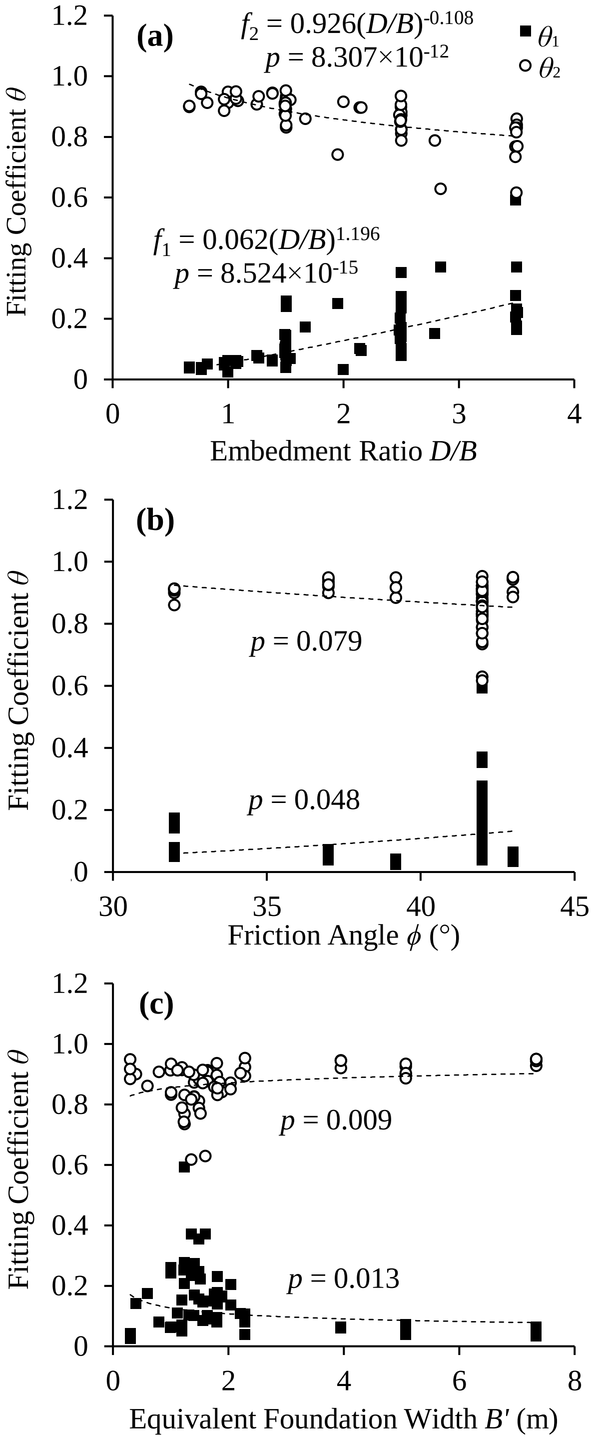

Figure 3.8 Relationship between the hyperbolic fitting coefficients and the foundation design parameters: (a) embedment ratio; (b) friction angle; (c) equivalent foundation width.

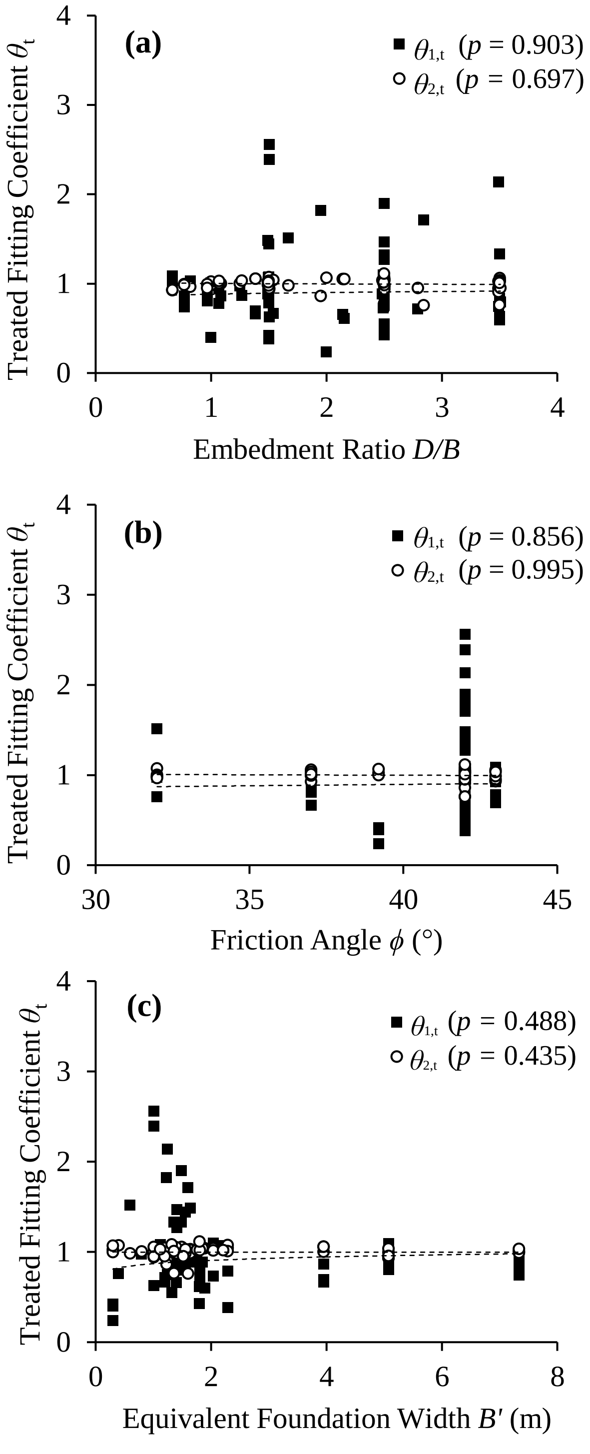

Figure 3.9 Relationship between the treated hyperbolic fitting coefficients and the foundation design parameters: (a) embedment ratio; (b) friction angle; (c) equivalent foundation width.

3.6.2 Correlation Structure of the Fitting Coefficients

In addition to the statistical dependency between the fitting coefficients and the foundation design parameters, the correlation between the treated coefficients $\theta_{1,t}$ and $\theta_{2,t}$ was assessed. The coefficients showed a strong correlation, with the Kendall's tau coefficient of ρ_τ=-0.563 and the associated p-value of 1.51×10^{-10}. The observed correlation structure was characterised by using copula theory, which is useful for modelling the nonlinear correlation between the fitting coefficients of the load-displacement curves [18]–[20], [87]. The Multivariate Copula Analysis Toolbox (MvCAT), developed by Sadegh, Ragno, and AghaKouchak (2017), was used to identify the copula function that best fits the correlation. The MvCAT utilises Bayesian analysis with Markov Chain Monte Carlo (MCMC) simulations, which allows for robust analyses of the optimal copula [98]. The considered types of copulas are Gaussian, Frank, and Nelsen, all of which are capable of modelling negatively correlated variables. The performance of each copula was evaluated with the Akaike Information Criterion (AIC) and the Bayes Information Criterion (BIC). As shown in the copula analysis results (Table 3.3), the Frank copula had the highest performance in terms of all criteria. Thus, the correlation structure was described with the Frank copula and the corresponding MCMC copula parameter (α=-5.32).

Figure 3.10 shows the probability distributions of the treated fitting coefficients $\theta_{1,t}$ and $\theta_{2,t}$. Similar to the distributions that were previously shown in Figure 3.5, the lognormal and generalised extreme value distributions provided a reasonable fit to the distribution of $\theta_{1,t}$ and $\theta_{2,t}$, respectively. For the generalised extreme value distribution, the shape parameter k is negative (-0.51), indicating that the distribution can be considered as a Weibull (Type III) distribution.

Table 3.3 Analysis results for the best copula.

Rank	Best-Fit Copula			Copula Parameter α	
	Maximum Likelihood	AIC	BIC	MCMC	Local
1	**Frank**	**Frank**	**Frank**	**-5.32**	**-6.98**
2	Nelsen	Nelsen	Nelsen	-5.32	-5.32
3	Gaussian	Gaussian	Gaussian	-0.70	-0.75

The distributions were truncated at both sides to limit the range of allowable values. The truncation prevents the generation of extreme values, which may yield unrealistic load-displacement curves and unnecessary conservatism in the estimated foundation reliability [16], [99]. The distributions of the coefficient were left-truncated by the minimum value of the coefficient and right-truncated by the maximum value, giving the allowable range of $\theta_{1,t}$=[0.237, 2.560] and $\theta_{2,t}$=[0.760, 1.115]. The three-sigma rule could also be used for the truncation, where the range is limited to the mean plus or minus three times the standard deviation; however, this gives the range of $\theta_{1,t}$=[-0.389, 2.369], which underestimates the boundaries and yields negative values that are unrealistic, and $\theta_{2,t}$=[0.808, 1.192] which overestimates the boundaries. Nevertheless, the boundary values from the two truncation methods do not deviate significantly from each other. Thus, the maximum and minimum values were used for the truncation, as it is seen to be more representative of the general boundaries of the obtained distributions.

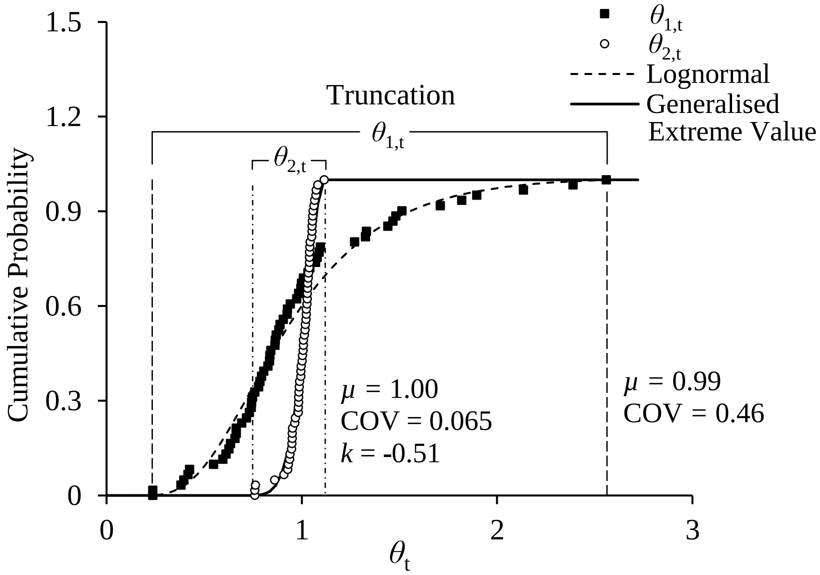

Figure 3.10 Sample and fitted cumulative probability distributions of the treated fitting coefficients.

3.6.3 Evaluation of the Obtained Statistical Characteristics

The selected copula and the obtained probability distributions of $\theta_{1,t}$ and $\theta_{2,t}$ were used to simulate the treated fitting coefficients (Figure 3.11) and the normalised load-displacement curves (Figure 3.12). The simulated curves were obtained by back-transforming the simulated fitting coefficients with *D/B*=2, which is approximately the average and median value for the foundations in the database. In general, it is shown that the coefficients and curves obtained from the database are well-encapsulated by the simulated data. The Kendall's tau coefficients in Figure 3.11 demonstrate that the correlation between the fitting coefficients from the simulated data ($\rho_{\tau,\text{sim}}$=-0.541) closely approximates the correlation from the database (ρ_τ=-0.563). Moreover, the probability distribution parameters of the simulated coefficients were nearly identical to those obtained from the database (Table 3.4), which indicates that the simulation outputs are consistent with the input parameters. This shows that the use of the selected copula, probability distributions, and regression functions ($f(D/B)$) are feasible for the simulation of the compiled load-displacement curves.

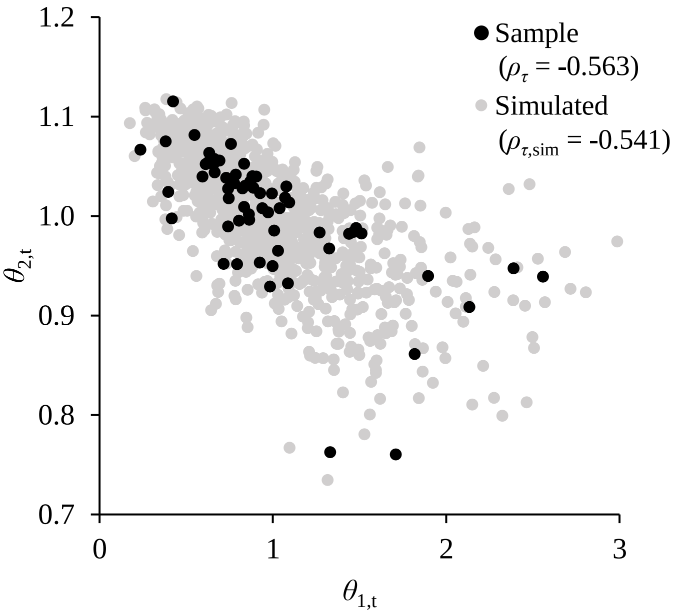

Figure 3.11 Simulated correlation between the treated fitting coefficients (1000 simulations).

It is noted that the fitting process leads to an extrapolation of the measured curves that do not reach large displacements. Thus, the fitted curves may not be fully representative of the actual load-displacement behaviour of the foundation for larger displacement levels; thus, further compilation of the load-displacement curves with larger displacements would be required for a more accurate characterisation of the load-displacement curves of the foundation. Due to the limited number of available load-displacement curves in the literature, the fitted hyperbolic curves were assumed to be representative of the measured curves in this study.

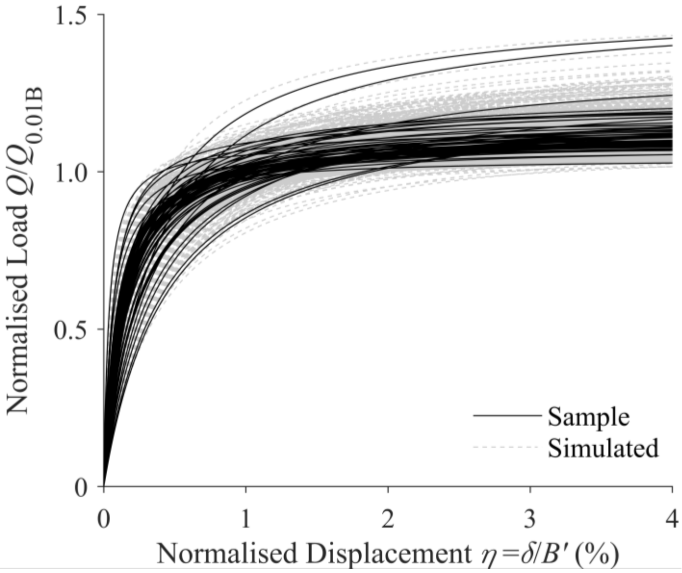

Figure 3.12 Simulated load-displacement curves with the coefficients back-transformed with D/B=2 (1000 simulations).

Table 3.4 Comparison of the probability distribution parameters between the simulated and obtained hyperbolic model coefficients (1000 simulations).

Coefficient	Mean		COV		Shape parameter k	
	Simulated	Obtained	Simulated	Obtained	Simulated	Obtained
$\theta_{1,\mathrm{t}}$	0.98	0.99	0.45	0.46	-	-
$\theta_{2,\mathrm{t}}$	1.00	1.00	0.061	0.065	-0.52	-0.51

Chapter 4. Reliability Simulations and LRFD Calibration

4.1. Overview

The probability of failure (p_f) and the associated reliability (β) of the foundation were estimated via reliability-based simulations of the load-displacement curves. In this study, the load and resistance factor design (LRFD) approach was adopted for the calibration of the resistance factor (ψ), which is applied to the computed foundation resistance to ensure that the foundation fulfils the targeted level of reliability (β_T). The reliability analysis and LRFD calibration were carried out for both the ultimate and serviceability limit states to allow for the comparison of the foundation reliability at each limit state. The analysis specifically considers the context of transmission tower foundations, as their design is often governed by the uplift loading conditions [4], [5]. It is noted that the spatial correlation of the soil properties was not considered in this study, while it can influence the performance and reliability of geotechnical structures, including foundations [100]–[102].

4.2. LRFD Framework and Performance Functions

The LRFD framework considers the following inequality, where the factored foundation capacity is greater than the factored loads.

$$\psi R_{\mathrm{n}} \geq \sum \gamma_i Q_{i,\mathrm{n}} \qquad \text{(Eq. 4.1)}$$

where ψ ($\leq$1) is the resistance factor, R_n is the nominal resistance, and γ_i ($\geq$1) is the load factor applied to the nominal load $Q_{i,n}$. The nominal resistance is taken as the calculated uplift capacity of the foundation (R_n=Q_{uc}).

For transmission tower foundations, the loads that induce uplift loads are mainly the wind loads Q_{WL}, and the dead loads Q_{DL} that are caused by differential wire tension. Thus, Equation 4.1 is rewritten as

$$Q_{\mathrm{uc}} = \frac{1}{\psi}\left(\gamma_{\mathrm{DL}} Q_{\mathrm{DL,n}} + \gamma_{\mathrm{WL}} Q_{\mathrm{WL,n}}\right) \qquad \text{(Eq. 4.2)}$$

where the subscripts DL and WL denote the dead loads and wind loads that induce uplift loads, respectively. The load factors γ_{DL}=1.25 and γ_{WL}=1.00 were applied, according to the AASHTO LRFD load combination limit state category, Strength III, which relates to structures exposed to high wind speeds [1].

4.2.1 SLS Performance Function

The performance functions for the SLS and ULS were defined by incorporating Equation 4.2. For the SLS, the performance function is

$$g = Q_{\mathrm{all}} - Q_{\mathrm{app}} = Q_{\mathrm{all}} - \left(\lambda_{\mathrm{DL}} Q_{\mathrm{DL,n}} + \lambda_{\mathrm{WL}} Q_{\mathrm{WL,n}}\right) \qquad \text{(Eq. 4.3)}$$

where λ is the bias, defined as the ratio between the measured and expected value of the associated parameter. The allowable load Q_{all} is a function of all sources of uncertainties in the load-displacement curves that are considered in this paper, as expressed in Equation 4.4.

$$Q_{\mathrm{all}} = M_{\mathrm{ULS}} M_{\mathrm{fit}} M_{\mathrm{SLS}} Q_{\mathrm{uc}} \qquad \text{(Eq. 4.4)}$$

The SLS model factor M_{SLS} is defined as

$$M_{\mathrm{SLS}} = \frac{\eta_{\mathrm{all}}}{\theta_1 + \theta_2 \eta_{\mathrm{all}}} = \frac{\eta_{\mathrm{all}}}{f_1 \theta_{1,\mathrm{t}} + f_2 \theta_{2,\mathrm{t}} \eta_{\mathrm{all}}} \qquad \text{(Eq. 4.5)}$$

where η_{all} is the allowable pseudo-strain (=δ_{all}/B'), and f_1 and f_2 are functions of the embedment ratio (*D/B*), obtained from the regression analysis in Figure 3.8a. Combining Equations 4.2, 4.4–4.5 gives the final form of the SLS performance function of

$$g = M_{\mathrm{ULS}} M_{\mathrm{fit}} \left(\frac{\eta_{\mathrm{all}}}{f_1 \theta_{1,\mathrm{t}} + f_2 \theta_{2,\mathrm{t}} \eta_{\mathrm{all}}}\right)\left(\frac{\gamma_{\mathrm{DL}} + \gamma_{\mathrm{WL}}\omega}{\psi_{\mathrm{SLS}}}\right) - (\lambda_{\mathrm{DL}} + \lambda_{\mathrm{WL}}\omega) \qquad \text{(Eq. 4.6)}$$

where ω is the ratio of the wind loads to the dead loads (=$Q_{\mathrm{WL,n}}/Q_{\mathrm{DL,n}}$). Since ω is unknown, ω=10 was assumed, as it was shown to be the value where the calibration outputs reach convergence [75].

4.2.2 Performance Function for the Evaluation of the Relationship between the SLS and ULS

For the ULS, failure occurs when the applied loads exceed the ultimate capacity of the foundation (Q_u) which is interpreted from the load-displacement curve. Hence, the performance function for the ULS is

$$g = Q_{\mathrm{u}} - Q_{\mathrm{app}} = \left(\frac{\gamma_{\mathrm{DL}} + \gamma_{\mathrm{WL}}\omega}{\psi_{\mathrm{ULS}}}\right) M^{*}_{\mathrm{ULS}} - (\lambda_{\mathrm{DL}} + \lambda_{\mathrm{WL}}\omega) \qquad \text{(Eq. 4.7)}$$

where M^{*}_{ULS} is the capacity model factor of the interpreted ultimate capacity of the foundation ($=Q_{int}/Q_{uc}$). It is to be noted that the interpreted foundation capacity Q_{int} is decided by the designer (e.g. peak load, tangent intersection load), which means that Q_{int} is not necessarily equal to Q_{ref}. For simplicity purposes, it was assumed that $Q_{int}=Q_{ref}$ and $M^{*}_{ULS}=M_{ULS}$ in this paper.

Finally, another performance function was defined to assess the probability of the foundation reaching the ULS, when the foundation displacement reaches the allowable displacement level that corresponds to the SLS condition (Equation 4.8).

$$g = Q_{\mathrm{u}} - Q_{\mathrm{all}} = M^{*}_{\mathrm{ULS}} - \left(\frac{\eta_{\mathrm{all}}}{\theta_1 + \theta_2\eta_{\mathrm{all}}}\right) M_{\mathrm{fit}} M_{\mathrm{ULS}} \qquad \text{(Eq. 4.8)}$$

The estimated probability from Equation 4.8 can be used to aid the design of the foundation-structure system, where the reliability of different components of the system needs to be controlled. This would allow for the coordination of the failure sequences, as referred to by several transmission structure design guidelines including ASCE-74 [103] and IEC 60826 (BSI 2017). Generally, it is recommended that the foundations have a higher level of reliability than the supported structure, since the repair costs are generally higher for foundations [55].

4.3. LRFD Calibration

4.3.1 Reliability Analysis Procedures and Input Parameters

The reliability analysis was run by generating 500,000 samples through MCS with the probability characteristics of the input parameters, summarised in Table 4.1. Regarding the applied loads, the probability characteristics from past literature were adopted for the dead loads [104], [105], and wind loads [75], [106]. Samples of the treated hyperbolic fitting coefficients $\theta_{1,t}$ and $\theta_{2,t}$ were generated with the truncated probability distributions and selected copula function. The generated coefficients were then back-transformed to θ_1 and θ_2 with a deterministic value of *D/B*.

Table 4.1 Summary of the input parameters for the reliability simulations.

Parameter	Distribution Type	Mean λ	COV	Truncation
λ_{DL}	Normal	1.05	0.10	-
λ_{WL}	Type I (Gumbel)	0.78	0.37	-
$\theta_{1,\mathrm{t}}$	Lognormal	0.99	0.46	[0.237, 2.560]
$\theta_{2,\mathrm{t}}$	Generalised Extreme Value	1.00	0.07	[0.760, 1.115]
η_{all}	Lognormal	0.05%, 0.10%,…, 3.90%	0.20	-
M_{ULS} [1]	Lognormal	1.67	0.55	-
M_{fit}	Lognormal	(Obtained from Figure 3.4: Hyperbolic Model) [2]		-

[1] The model statistics of the selected reference load $Q_{0.01\mathrm{B}}$ (Figure 3.7) were applied.

[2] Mean and COV at each normalised displacement level applied to the corresponding allowable displacement level.

The allowable pseudo-strain η_{all} was treated as a random variable, instead of a deterministic value, to account for the uncertainties in η_{all}. This is because the value of η_{all} or δ_{all} is affected by various factors, such as the soil-foundation-structure interaction and the uniformity of settlement, which leads to inconsistencies and uncertainties in η_{all} [24]. Specifically for foundations in sands, Najjar et al. [107] derived the statistics of the allowable displacement as a lognormal variable, with the mean of 50mm and COV of 0.2, by analysing the data by Skempton and Macdonald [108]. Based on this, COV(η_{all})=0.2 was adopted for the range of considered η_{all}=0.05–3.90%, which corresponds to the foundation widths of approximately 1–10m for the allowable displacement of 50mm. The upper limit of η_{all} was set as 3.90%, as the fitting model factor M_{fit} could not be obtained at higher η values, due to insufficient data with larger displacements. It is noted that the criteria for the differential settlements or rotation were not considered, as this study considers the displacement of a single foundation.

4.3.2 Target Reliability Index

For the calibration of the SLS resistance factor (ψ_{SLS}), the SLS target reliability index of β_{SLS}=2.33 was chosen, which corresponds to p_f=1%. A lower β_{SLS} may be allowed, since the exceedance of the SLS leads to relatively small consequences of failure, compared to the ULS [12], [21]. The target reliability index of β_{SLS}=1 was suggested by Meyerhof [109] and Kulicki et al. [14] for the SLS design of foundations. In addition, the parametric studies by Phoon et al. [21] demonstrated that the reliability of the foundation did not exceed β=2 for spread foundations under drained uplift loading, given that δ_{all}=25mm and D/B=2. Nevertheless, the target reliability index of β_{SLS}=2.33 was adopted for the LRFD calibration, as it has been commonly applied for baseline studies in the literature about the RBSLS design of foundations [16]–[18], [20], [78].

4.3.3 LRFD Calibration Results

The calibrated resistance factors ψ_{SLS} for each allowable displacement η_{all} are presented in Figure 4.1. As shown, ψ_{SLS} has a hyperbolic relationship with η_{all}, which tended to plateau and reach convergence at approximately ψ_{SLS}=0.54 with further increases in η_{all}. Moreover, the value of D/B had significant effects on ψ_{SLS}, where a higher D/B leads to lower ψ_{SLS} at relatively small η_{all} values (≤1.5%) and higher ψ_{SLS} at large η_{all} values (>1.5%).

The effects of the fitting errors on the calibrated ψ_{SLS} were assessed in Figure 4.2, and it was shown that the incorporation of the fitting model factor M_{fit} yielded lower ψ_{SLS} values. Such effects were more pronounced at relatively low η_{all} values of less than 0.2%, which may be due to the higher COV in M_{fit} at this range of η. This implies that the fitting errors may have more significant effects on the calibration results for foundations with large widths, which have smaller η_{all} for a given δ_{all} value. From this, it was deduced that the consideration of the statistical dependencies on D/B and the fitting errors led to improved accuracy of the calibration results.

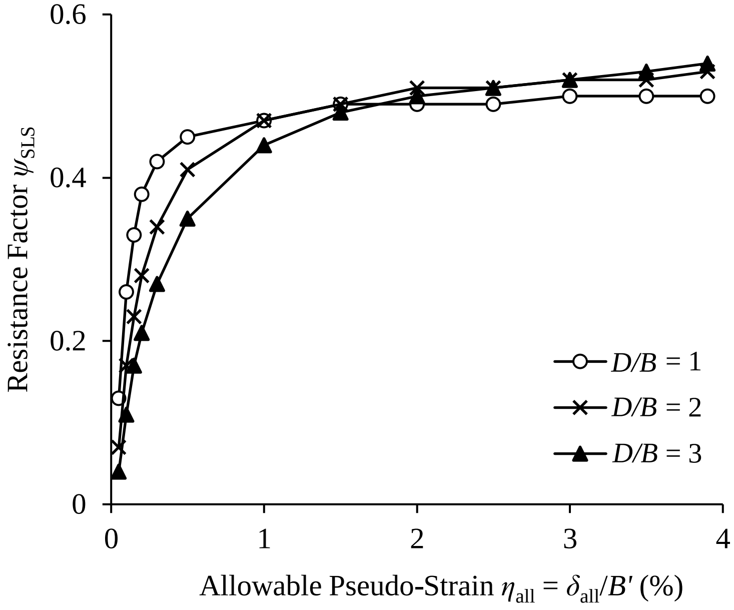

Figure 4.1 Effects of the embedment ratio (D/B) on the relationship between the calibrated SLS resistance factor (ψ_{SLS}) and allowable pseudo-strain (η_{all}).

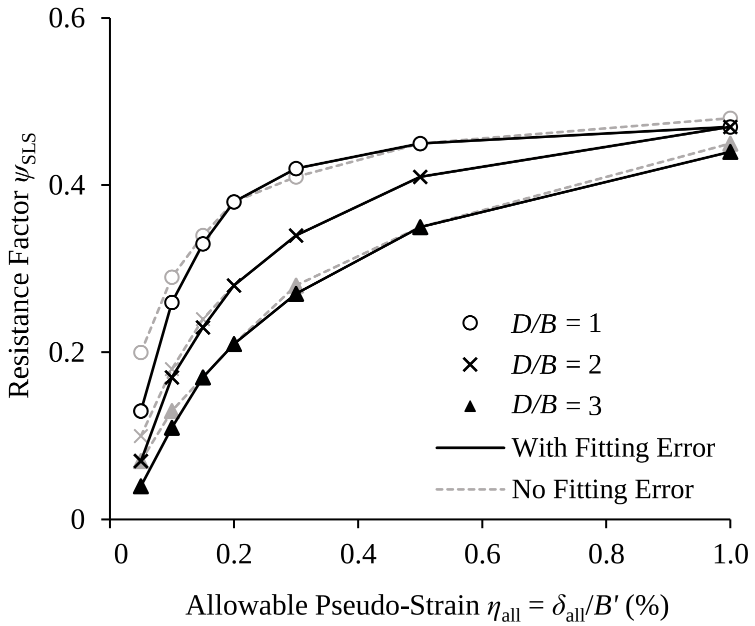

Figure 4.2 Effects of the fitting model factor (M_{fit}) on the calibrated SLS resistance factor (ψ_{SLS}).

4.4. Assessment of the Relationship Between the Foundation Reliability at the ULS and SLS

4.4.1 Governing Limit State and Limiting Allowable Pseudo-Strain η_{all}

The design of foundations generally requires a higher level of reliability to be fulfilled against ULS failure, compared to SLS failure [12], [21]. To ensure that the foundation fulfils both limit states, the governing limit state needs to be identified and determined for the design. The ULS resistance factor ψ_{ULS} was calibrated and compared with the SLS resistance factor ψ_{SLS} to determine governing limit state for design at each η_{all} value. The limit state that gives a smaller resistance factor was considered as the governing limit state. The calibration of ψ_{ULS} was carried out with the performance function in Equation 4.7 and the target reliability indices of β_{ULS}=2.3–3.2 which correspond to the range of values that are implicit in the existing designs for spread foundations under drained uplift conditions [21].

Figure 4.3 shows an example of determining the governing limit state through the comparison of ψ_{SLS} and ψ_{ULS}. In the figure, it is shown that the SLS is the governing limit state for small η_{all} values ($\psi_{SLS}<\psi_{ULS}$). With further increases in η_{all}, the value of ψ_{SLS} eventually exceeds ψ_{ULS}, causing the ULS to become the governing limit state. The upper limit of η_{all}, where the SLS governs the design, is referred to as the limiting allowable pseudo-strain (η_{lim}) in this study. As illustrated in Figure 4.4, η_{lim} can also be interpreted as the allowable pseudo-strain η_{all} with a 1% probability of exceedance (β_{SLS}=2.33), when the ULS resistance factor is used for design. Since ψ_{ULS} is interpreted as the upper limit of the resistance factor, it is implied that η_{lim} is the maximum design value of η_{all} in the RBSLS design. Figure 4.4 presents the value of η_{lim} for each ULS target reliability index β_{ULS}. It is demonstrated that the value of η_{lim} decreases with an increase in β_{ULS}. The observed relationship is as expected, as a higher β_{ULS} results in the calibration of a smaller ψ_{ULS} which corresponds to lower η_{all} values. For each curve that is shown in Figure 4.4, the area above the curve ($\eta_{all} > \eta_{lim}$) can be interpreted as the domain, where a constant value of ψ_{ULS} is applied to the calculated resistance of the foundation. For the area below the curve ($\eta_{all} < \eta_{lim}$), the corresponding value of ψ_{SLS} is used.

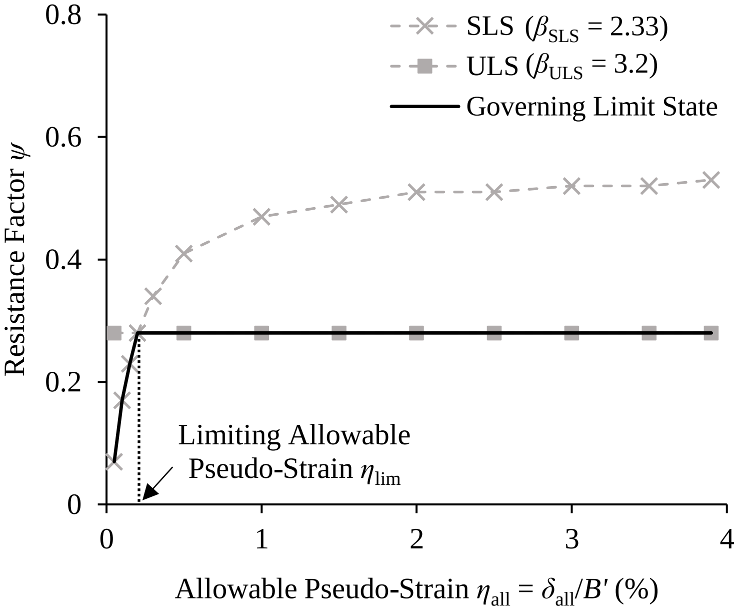

Figure 4.3 Determination of the limiting allowable pseudo-strain (η_{lim}) and the governing limit state.

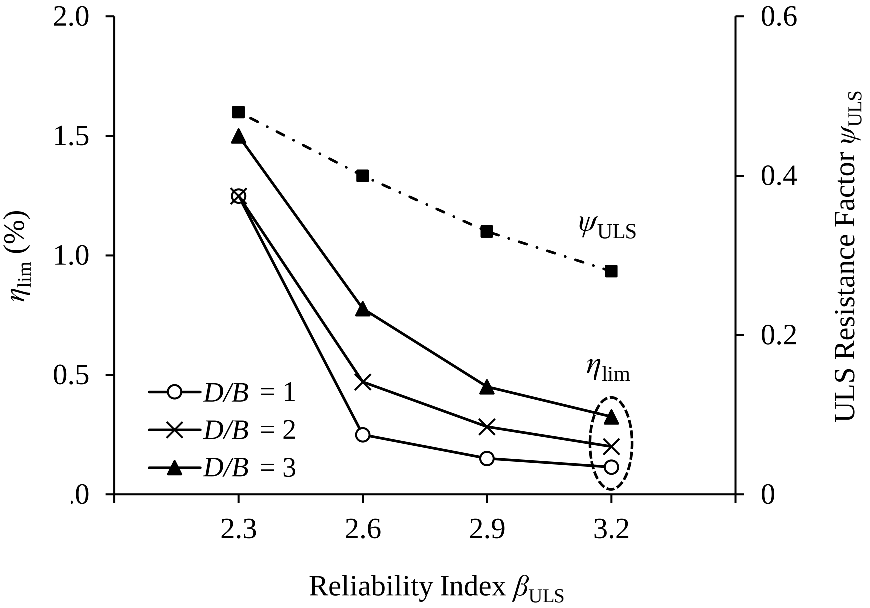

Figure 4.4 Values of the limiting allowable pseudo-strain (η_{lim}) and ULS resistance factor (ψ_{ULS}) for different ULS target reliability index (β_{ULS}) values.

4.4.2 Probability of ULS Failure at the SLS Condition

While the foundation design can be carried out by considering a single governing limit state, additional analysis was carried out to assess the probability of the ULS being reached, when the foundation reaches the SLS condition, or the allowable displacement level (δ_{all} or η_{all}). This can be expressed as the probability of the allowable load (Q_{all}) being greater or equal to the ultimate foundation capacity (Q_u), written as $P(Q_{all} \geq Q_u)$. With the estimated $P(Q_{all} \geq Q_u)$, the reliability of the foundation against ultimate failure could be compared with the reliability of the supported structural components for a given serviceability requirement. The obtained relative reliability could be used to evaluate the suitability of the foundation design and the design value of η_{all}. It is noted that this probability is essentially equal to $P(Q_{all}=Q_u)$ when the peak load of the foundation is interpreted as Q_u, as further increases in the mobilised loads would not be possible. On the other hand, if a different capacity such as Q_{TIU} was interpreted as Q_u, the allowable load Q_{all} could exceed Q_u at large allowable displacement levels.

Figure 4.5 shows the probability $P(Q_{all} \geq Q_u)$, computed with the performance function in Equation 4.8, for each allowable pseudo-strain level. It was observed that

$P(Q_{all} \geq Q_u)$ increases exponentially with an increase in the η_{all} that is reached by the foundation, up to the point of approximately η_{all}=1%. The plateau is reached where $P(Q_{all} \geq Q_u)$ is nearly equal to 100%, which indicates that $Q_{all} \approx Q_u$. The plateau may have been reached at a different value of $P(Q_{all} \geq Q_u)$, if a different interpreted capacity Q_{int} was used as Q_u. Nevertheless, it is shown that the likelihood of the joint occurrence of ULS and SLS failures increases significantly, as the allowable load Q_{all} approaches the ultimate failure capacity Q_u of the foundation.

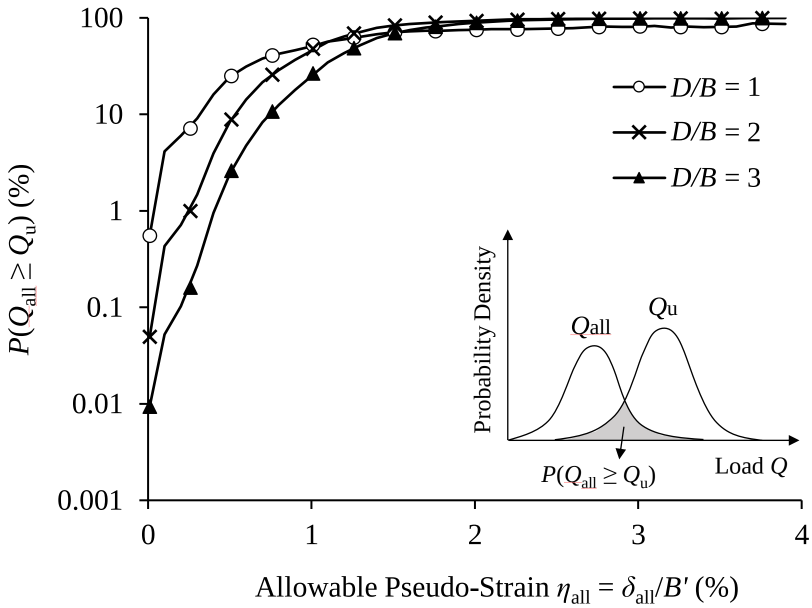

Figure 4.5 Probability of the allowable load (Q_{all}) exceeding the ultimate foundation capacity (Q_u).

Chapter 5. Proposed RBSLS Design Procedures

5.1. Proposed Procedures

The RBSLS design procedures of determining the design resistance factor ψ_d and design foundation capacity Q_d were proposed, as presented in Figure 5.1. In addition to the fundamental framework of selecting an appropriate SLS resistance factor, the proposed procedures include the determination of the governing limit state and the evaluation of the probability $P(Q_{all} \geq Q_u)$.

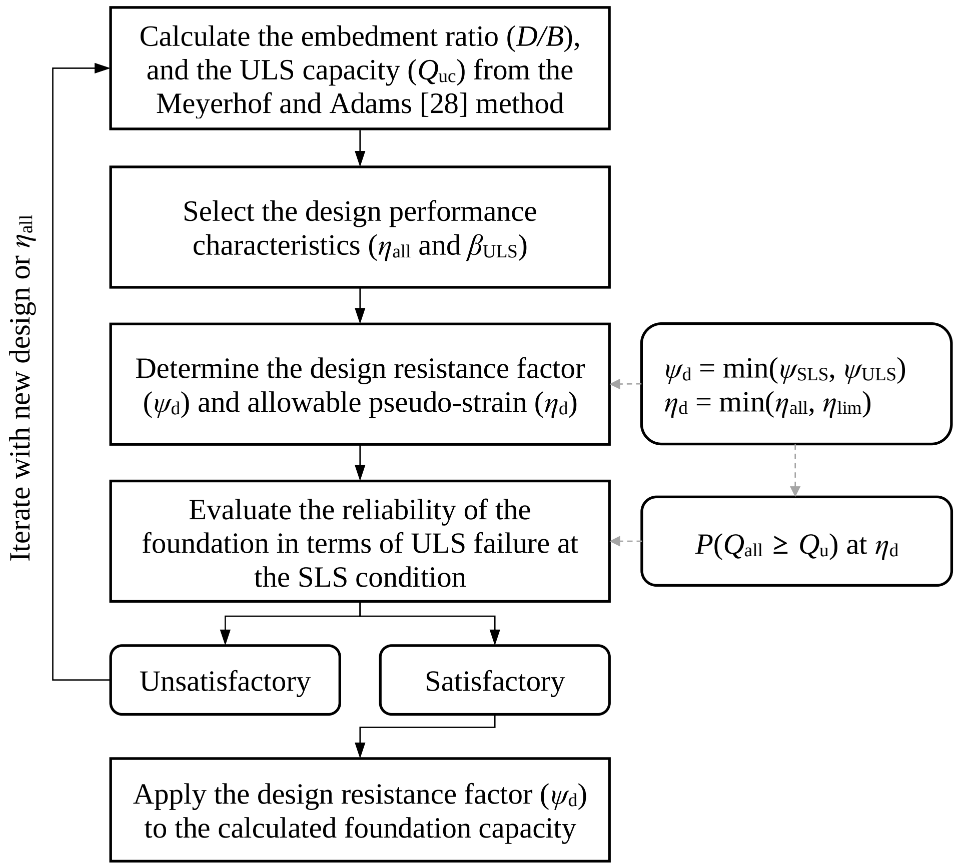

Figure 5.1 Proposed reliability-based SLS design procedures for estimating the design foundation capacity (Q_d) of spread foundations under uplift loading in cohesionless soils.

5.2. Example of the RBSLS Design Procedures

An example is provided to demonstrate the use of the procedures to obtain the design foundation capacity that fulfils the target reliability of the SLS (β_{SLS}=2.33) and ULS (β_{ULS}=2.3–3.2). The example considers a square shallow foundation of a transmission tower with the width and embedment depth of 3m which corresponds to the embedment ratio of D/B=1. The nominal allowable displacement was assumed to be 50mm which gives the η_{all}=1.48%, considering that the circular equivalent width of the foundation is 3.39m. The ULS target reliability was taken as β_{ULS}=3.2, which is recommended for the ULS design of transmission tower foundations (Phoon, Kulhawy, and Grigoriu 2003). The key steps of the procedures for determining the design foundation capacity are described as follows:

1. Compute the ultimate uplift capacity of the foundation Q_{uc} by using the Meyerhof and Adams [28] method with the design foundation dimensions and soil properties.
2. Obtain the resistance factors ψ_{SLS} and ψ_{ULS} by considering the selected design performance characteristics, η_{all} and β_{ULS}, and the embedment ratio D/B. Then, determine the design resistance factor ψ_d that relates to the governing limit state which gives a smaller ψ value, and the corresponding allowable pseudo-strain η_d. As obtained from Figures 4.1 and 4.4, the resistance factors are ψ_{SLS}=0.49 and ψ_{ULS}=0.28, which gives ψ_d=0.28. Since the ULS governs ($\psi_{ULS}<\psi_{SLS}$), the ULS resistance factor is applied, and the allowable pseudo-strain is capped at $\eta_d=\eta_{lim}$=0.11% (δ_{all}=3.73mm).
3. With the obtained η_d, estimate $P(Q_{all}\geq Q_u)$. From Figure 4.5, $P(Q_{all}\geq Q_u)$=4.3% for η_d=0.11%. This can be used to evaluate the estimated reliability of the foundation, relative to other components in the foundation-structure system, given that the foundation displacement reached the SLS condition. As a general guidance based on the ASCE-74 guidelines [103], it could be checked that probability of ULS failure of the foundation $P(Q_{all}\geq Q_u)$ is one magnitude smaller than the probability of failure of the transmission structure.
4. If the evaluated relative reliability of the foundation is satisfactory, calculate the design foundation capacity by using the determined resistance factor

(Q_d=$\psi_d Q_{uc}$). If unsatisfactory, reiterate from Step (1) with a different foundation design or design performance characteristics. Assuming that the foundation reliability is satisfactory, the resulting design foundation capacity Q_d=0.28Q_{uc} for this example.

With the estimated design foundation capacity, it is checked whether the foundation satisfies the LRFD equation of $\psi_{\mathrm{d}} Q_{\mathrm{uc}} = Q_{\mathrm{d}} \geq 1.4 Q_{\mathrm{DL,n}} + Q_{\mathrm{WL,n}}$ from the AASHTO Strength III load combination limit state category that was adopted for the calibration [1].

Chapter 6. Conclusion and Suggestions

6.1 Conclusion

In this paper, a reliability-based design approach was developed for the SLS design of spread foundations under uplift loading in cohesionless soils. The uncertainties in the compiled load-displacement curves were quantified to estimate the foundation reliability by using MCS, and to calibrate the SLS resistance factors for different allowable displacement levels within the LRFD framework. Additional statistical considerations were investigated, including the fitting errors of the empirical model and the statistical dependencies in the fitting coefficients, as well as their effects on the calibrated resistance factors.

For the normalisation of the load-displacement curves, it was shown that the normalisation of the loads by the slope tangent capacity with the offset of 0.01*B* resulted in the least scatter in the curves. In terms of the SLS model, the hyperbolic model provided a better fit to the normalised curves, compared to the power law model, as demonstrated by the relatively low RMSE values and fitting errors. The hyperbolic fitting coefficients showed a strong statistical dependency on the embedment ratio of the foundation (*D/B*), which were treated by regressing the fitting coefficients against *D/B*.

The LRFD calibration was carried out with the target reliability index of β_{SLS}=2.33 (1% probability of exceedance), and the results showed a nonlinear relationship between the resistance factors and the allowable pseudo-strain η_{all}. The relationship was shown to be significantly affected by the *D/B* of the foundation. The incorporation of the fitting errors resulted in lower resistance factors for small η_{all} (<0.2%), due to the higher fitting errors in this range of η_{all}. From this, it was deduced that the consideration of the statistical dependencies and fitting errors resulted in improved accuracy of the calibration results.

The relationship of the SLS with the ULS was explored, and the concept of the limiting allowable pseudo-strain η_{lim} was suggested to define the upper limit of the η_{all} value, where the SLS governs the design. Moreover, this study assessed the probability of the ultimate failure being reached at the SLS condition of the foundation, where the allowable load exceeds the ultimate capacity. Preliminary results have been presented, which can be used to evaluate the relative reliability of the foundation in the overall foundation-structure system for a given SLS criteria.

With consideration of the obtained relationship between the ULS and SLS, the procedures for determining the design foundation capacity were proposed, along with an example that demonstrated each step of the procedures.

6.2 Suggestions for Further Work

For the development of RBSLS design methods, an accurate characterisation of the load-displacement behaviour and foundation reliability is crucial. Since the analyses in this study are based on the compiled database and several assumptions, additional work could be carried out to extend the research further and to improve the accuracy of the analysis outcomes. The suggestions for further work are as follows:

1. Further adjustments of the reliability analysis outputs may be required with the introduction of additional load test data and the use of project-specific calibration inputs. Particularly, load-displacement curves with large maximum displacement levels would be required to improve the accuracy of the analysis results for large allowable displacement levels.
2. As the spatial variability and correlation in the soil properties were not considered in this paper, further studies could be carried out to incorporate spatial parameters in the development of the RBSLS design method.
3. Additional studies could be carried out to quantify the uncertainties in the allowable displacement or pseudo-strain η_{all}, specifically for spread foundations under uplift loading conditions in cohesionless soils. This would require the assessment of the limit state requirements of the structure, and the relevant criteria for differential settlement and angular displacements that may occur due to the uplift. The obtained probability distributions of η_{all} could be used to yield more project-specific resistance factors.
4. Different values of the interpreted ultimate capacity can be used to assess the probability of ULS failure at the SLS condition $P(Q_{all} \geq Q_u)$ to provide more practical results that can be used to assess the relative reliability of the foundation and structure.

References

[1] AASHTO, "AASHTO LRFD bridge design specifications 8th edition." AASHTO, Washington, D.C., 2017.

[2] CSA (Canadian Standards Association), "Canadian highway bridge design code." Canadian Standards Association (CSA), Ontario, Canada, 2014.

[3] BSI (British Standards Institution), "Eurocode 7: Geotechnical design - Part 1: General rules, BS EN 1997-1:2004." CEN, 2004.

[4] F. H. Kulhawy, C. H. Trautmann, J. F. Beech, T. D. O'Rourke, and W. McGuire, "Transmission line structure foundations for uplift-compression loading, EL-2870," Palo Alto, CA, 1983.

[5] IEEE, "IEEE guide for transmission structure foundation design and testing, IEEE Std 691-2001." Institute of Electrical and Electronics Engineers, New York, NY, 2001.

[6] F. Yang, J. Yang, J. Han, and Z. Zhang, "Study on the limited values of foundation deformation for a typical UHV transmission tower," *IEEE Trans. Power Deliv.*, vol. 25, no. 4, pp. 2752–2758, Oct. 2010, doi: 10.1109/TPWRD.2010.2045662.

[7] F. M. Levy and D. J. Richards, "Full scale rapid uplift tests on transmission tower footings," in *18th International Conference on Soil Mechanics and Geotechnical Engineering: Challenges and Innovations in Geotechnics, ICSMGE 2013*, 2013, vol. 4, pp. 2791–2794.

[8] J. Farkas and L. Marczal, "Foundation of a 157 m high transmission tower," *Period. Polytech. Civ. Eng.*, vol. 38, no. 1, pp. 29–40, Sep. 1994.

[9] T. L. L. Orr and E. R. Farrell, "Use of serviceability limit state calculations in geotechnical design," in *15th International Conference on Soil Mechanics and Foundation Engineering*, 2001, pp. 821–824.

[10] K. K. Phoon and J. V. Retief, *Reliability of Geotechnical Structures in ISO2394*, 1st ed. Leiden, The Netherlands: CRC Press, 2016.

[11] S. Zhang, L. Zhong, and Z. Xu, "Reliability of foundation pile based on settlement and a parameter sensitivity analysis," *Math. Probl. Eng.*, vol. 2016, pp. 1–7, 2016, doi: 10.1155/2016/1659549.

[12] N. C. Samtani and J. M. Kulicki, “Incorporation of foundation movements in AASHTO LRFD bridge design process Second edition, FHWA-HIF-18-007,” Washington, D.C., 2018.

[13] N. C. Samtani and T. M. Allen, “Expanded database for service limit state calibration of immediate settlement of bridge foundations on soil, FHWA-HIF-18-008,” Washington, D.C., 2018.

[14] J. M. Kulicki, W. G. Wassef, A. S. Nowak, D. R. Mertz, N. C. Samtani, and H. Nassif, “Bridges for service life beyond 100 years: Service limit state design, S2-R19B-RW-1,” Washington, D.C., D.C., 2015.

[15] K.-K. Phoon and F. H. Kulhawy, “Serviceability limit state reliability-based design,” in *Reliability-based design in geotechnical engineering: computations and applications*, 1st ed., K.-K. Phoon, Ed. Abingdon, Oxon: CRC Press, 2008, pp. 344–384.

[16] J. C. Huffman, A. W. Strahler, and A. W. Stuedlein, “Reliability-based serviceability limit state design for immediate settlement of spread footings on clay,” *Soils Found.*, vol. 55, no. 4, pp. 798–812, Aug. 2015, doi: 10.1016/j.sandf.2015.06.012.

[17] J. C. Huffman, J. P. Martin, and A. W. Stuedlein, “Calibration and assessment of reliability-based serviceability limit state procedures for foundation engineering,” *Georisk Assess. Manag. Risk Eng. Syst. Geohazards*, vol. 10, no. 4, pp. 280–293, Oct. 2016, doi: 10.1080/17499518.2016.1183797.

[18] S. C. Reddy and A. W. Stuedlein, “Serviceability limit state reliability-based design of augered cast-in-place piles in granular soils,” *Can. Geotech. J.*, vol. 54, no. 12, pp. 1704–1715, Dec. 2017, doi: 10.1139/cgj-2016-0146.

[19] A. W. Stuedlein and M. Uzielli, “Serviceability limit state design for uplift of helical anchors in clay,” *Geomech. Geoengin.*, vol. 9, no. 3, pp. 173–186, Jul. 2014, doi: 10.1080/17486025.2013.857049.

[20] C. Tang, K.-K. Phoon, D.-Q. Li, and S. O. Akbas, “Expanded database assessment of design methods for spread foundations under axial compression and uplift loading,” *J. Geotech. Geoenvironmental Eng.*, vol. 146, no. 11, p. 04020119, 2020, doi: 10.1061/(asce)gt.1943-5606.0002373.

[21] K. K. Phoon, F. H. Kulhawy, and M. D. Grigoriu, “Reliability-based design of foundations for transmission line structures, TR-105000,” Palo Alto, CA,

1995.

[22] Y. Wang and F. H. Kulhawy, "Reliability index for serviceability limit state of building foundations," *J. Geotech. Geoenvironmental Eng.*, vol. 134, no. 11, pp. 1587–1594, Nov. 2008, doi: 10.1061/(ASCE)1090-0241(2008)134:11(1587).

[23] S. G. Paikowsky *et al.*, "Load and resistance factor design (LRFD) for deep foundations, NCHRP Report 507," Washington, D.C., 2004.

[24] L. M. Zhang and A. M. Y. Ng, "Probabilistic limiting tolerable displacements for serviceability limit state design of foundations," *Géotechnique*, vol. 55, no. 2, pp. 151–161, Mar. 2005, doi: 10.1680/geot.2005.55.2.151.

[25] BSI (British Standards Institution), "Eurocode - Basis of structural design, BS EN 1990:2002." British Standards Institution, 2002.

[26] S. G. Paikowsky, M. C. Canniff, K. Lesny, A. Kisse, S. Amatya, and R. Muganga, "LRFD design and construction of shallow foundations for highway bridge structures, NCHRP Report 651," Washington, D.C., 2010.

[27] K.-K. Phoon, "Reliability-based design of foundations for transmission line structures," Cornell University, 1995.

[28] G. G. Meyerhof and J. I. Adams, "The ultimate uplift capacity of foundations," *Can. Geotech. J.*, vol. 5, no. 4, pp. 225–244, 1968, doi: 10.1139/t68-024.

[29] C. Tang and K.-K. Phoon, *Model Uncertainties in Foundation Design*, 1st ed. Boca Raton, FL: CRC Press, 2021.

[30] S. Mukherjee and G. L. Sivakumar Babu, "Reliability analysis of anchor foundations Subject to vertical uplift forces," *Indian Geotech. J.*, vol. 50, no. 6, pp. 982–993, Dec. 2020, doi: 10.1007/s40098-020-00442-2.

[31] J. M. Han, K.-Y. Gu, K.-S. Kim, S.-A. Jo, and S.-R. Kim, "Database classification for LRFD of spread foundations under uplift loading in cohesionless soils," *Probabilistic Eng. Mech.*, vol. 69, p. 103266, Jul. 2022, doi: 10.1016/j.probengmech.2022.103266.

[32] B. M. Das and S. K. Shukla, *Earth Anchors*, 2nd ed. Plantation, FL: J. Ross Publishing, Inc., 2013.

[33] D. Martin and A. Cochard, "Design of anchor plates," in *International Conference on Large High Voltage Electric Systems*, 1978, pp. 1–20.

[34] M. Dithinde, K. K. Phoon, M. De Wet, and J. V. Retief, "Characterization of

model uncertainty in the static pile design formula," *J. Geotech. Geoenvironmental Eng.*, vol. 137, no. 1, pp. 70–85, 2011, doi: 10.1061/(asce)gt.1943-5606.0000401.

[35] B. H. Fellenius, *Basics of Foundation Design*, Electronic. Sidney, Canada: www.Fellenius.net, 2021.

[36] A. Hirany and F. H. Kulhawy, "Conduct and interpretation of load tests on drilled shaft foundations, Volume 1: Detailed Guidelines, EPRI EL-5915," Palo Alto, CA, 1988.

[37] J. L. Withiam and F. H. Kulhawy, "Analysis procedure for drilled shaft uplift capacity," *Drilled Piers and Caissons*. American Society of Civil Engineers, New York, pp. 82–97, 1981.

[38] N. S. Mattes and H. G. Poulos, "Settlement of single compressible pile," *J. Soil Mech. Found. Div.*, vol. 95, no. 1, pp. 189–207, Jan. 1969, doi: 10.1061/JSFEAQ.0001217.

[39] Y.-J. Chen, H.-W. Chang, and F. H. Kulhawy, "Evaluation of uplift interpretation criteria for drilled shaft capacity," *J. Geotech. Geoenvironmental Eng.*, vol. 134, no. 10, pp. 1459–1468, Oct. 2008, doi: 10.1061/(ASCE)1090-0241(2008)134:10(1459).

[40] W. S. Housel, "Pile load capacity: Estimates and test results," *J. Soil Mech. Found. Div.*, vol. 92, no. 4, pp. 1–30, Jul. 1966, doi: 10.1061/JSFEAQ.0000887.

[41] T. D. O'Rourke and F. H. Kulhawy, "Observations on load tests on drilled shafts," *Proceedings of Drilled Piers and Caissons II*. American Society of Civil Engineers, pp. 113–128, 1985.

[42] E. E. de Beer, "Experimental determination of the shape factors and the bearing capacity factors of sand," *Géotechnique*, vol. 20, no. 4, pp. 387–411, Dec. 1970, doi: 10.1680/geot.1970.20.4.387.

[43] F. M. Fuller and H. E. Hoy, "Pile load tests including quick-load test method, conventional methods, and interpretations," *Highw. Res. Rec.*, no. 333, pp. 74–86, 1970.

[44] J. B. Hansen, "Discussion of 'Hyperbolic Stress-Strain Response: Cohesive Soils,'" *J. Soil Mech. Found. Div.*, vol. 89, no. 4, pp. 241–242, Jul. 1963, doi: 10.1061/JSFEAQ.0000542.

[45] J. B. Hansen, "Discussion of 'Hyperbolic Stress-Strain Response: Cohesive Soils,'" *J. Soil Mech. Found. Div.*, vol. 89, no. 4, pp. 241–242, Jul. 1963, doi: 10.1061/JSFEAQ.0000542.

[46] C. van der Veen, "The bearing capacity of a pile," 1953.

[47] F. K. Chin, "Estimation of the ultimate load of piles from tests not carried to failure," in *Proceedings of 2nd Southeast Asian Conference on Soil Engineering*, 1970, pp. 81–92.

[48] N. S. Mattes and H. G. Poulos, "Settlement of single compressible pile," *J. Soil Mech. Found. Div.*, vol. 95, no. 1, pp. 189–207, Jan. 1969, doi: 10.1061/JSFEAQ.0001217.

[49] F. H. Kulhawy, "Some observations on modeling in foundation engineering," in *Proceeding of the 8th International Conference on Computer Methods and Advances in Geomechanics (1)*, 1994, pp. 209–214.

[50] R. Frank *et al.*, "Designer's guide to Eurocode 7: Geotechnical design." Institute of Civil Engineers (ICE), London, UK, 2005.

[51] M. Dithinde, K. K. Phoon, M. De Wet, and J. V. Retief, "Characterization of model uncertainty in the static pile design formula," *J. Geotech. Geoenvironmental Eng.*, vol. 137, no. 1, pp. 70–85, 2011, doi: 10.1061/(ASCE)GT.1943-5606.0000401.

[52] IEEE, "National electrical safety code (NESC)." Institute of Electrical and Electronics Engineers, New York, NY, 2017.

[53] British Standards Institution, "BS IEC 60826:2017 Overhead transmission lines. Design criteria." British Standards Institution, London, UK, 2017.

[54] K. K. Phoon, "Reliability-based design incorporating model uncertainties," in *3rd International Conference on Geotechnical Engineering combined with 9th Yearly Meeting of the Indonesian Society for Geotechnical Engineering*, 2005, pp. 191–203.

[55] K.-K. Phoon, F. H. Kulhawy, and M. D. Grigoriu, "Reliability-based design for transmission line structure foundations," *Comput. Geotech.*, vol. 26, no. 3–4, pp. 169–185, 2000, doi: 10.1016/S0266-352X(99)00037-3.

[56] D. Essery, T. P. Taylor, and M. El-Sharnouby, "Comparison between AASHTO and CHBDC design methods for MSE retaining wall and its implications on transportation agencies," in *Conference of the Transportation*

Association of Canada, 2017, pp. 40–42.

[57] J. M. Duncan, "Factors of safety and reliability in geotechnical engineering," *J. Geotech. Geoenvironmental Eng.*, vol. 126, no. 4, pp. 307–316, 2000.

[58] F. H. Kulhawy, K.-K. Phoon, W. A. Prakoso, and A. Hirany, "Reliability-based design of foundations for transmission line structures," in *Electrical Transmission Conference*, 2006, pp. 184–194.

[59] A. Zhou, N. Post, R. Pingry, J. Cain, J. J. Lesko, and S. W. Case, *Durability of composites under fatigue loads*. Woodhead Publishing, 2007.

[60] T. M. Allen, A. S. Nowak, and R. J. Bathurst, "Calibration to determine load and resistance factors for geotechnical and structural design, Circular E-C079," Washington, D.C., 2005.

[61] G. B. Baecher and J. T. Christian, *Reliability and statistics in geotechnical engineering*, 1st ed. Chichester, England: John Wiley & Sons Ltd., 2003.

[62] K.-K. Phoon, F. H. Kulhawy, and M. D. Grigoriu, "Development of a reliability-based design framework for transmission line structure foundations," *J. Geotech. Geoenvironmental Eng.*, vol. 129, no. 9, pp. 798–806, 2003, doi: 10.1061/(ASCE)1090-0241(2003)129:9(798).

[63] R. J. Bathurst, T. M. Allen, and A. S. Nowak, "Calibration concepts for load and resistance factor design (LRFD) of reinforced soil walls," *Can. Geotech. J.*, vol. 45, no. 10, pp. 1377–1392, 2008, doi: 10.1139/T08-063.

[64] I. Stipanovic *et al.*, "Performance goals for roadway bridges of COST ACTION TU 1406 - WG2," 2017. doi: 10.13140/RG.2.2.31072.94721.

[65] R. M. Barker, J. M. Duncan, K. B. Rojiani, P. S. K. Ooi, C. K. Tan, and S.-G. Kim, "Manuals for the design of bridge foundations: Shallow foundations, driven piles, retaining walls and abutments, drilled shafts, estimating tolerable movements, and load factor design specifications and commentary," Washington, D.C., 1991.

[66] G. Kim and J. Lee, "Load and resistance factor design for serviceability limit state of laterally loaded drilled shafts for transmission line structures in sands," *J. Geotech. Geoenvironmental Eng.*, vol. 148, no. 1, Jan. 2022, doi: 10.1061/(ASCE)GT.1943-5606.0002711.

[67] D. Padmanabhan, H. Agarwal, J. E. Renaud, and S. M. Batill, "A study using Monte Carlo Simulation for failure probability calculation in Reliability-

Based Optimization," *Optim. Eng.*, vol. 7, no. 3, pp. 297–316, Sep. 2006, doi: 10.1007/s11081-006-9973-8.

[68] C. Huang, A. El Hami, and B. Radi, "Overview of structural reliability analysis methods — Part I : Local reliability methods," *Incert. fiabilité des systèmes multiphysiques*, vol. 17, no. 1, Feb. 2017, doi: 10.21494/ISTE.OP.2017.0115.

[69] R. E. Melchers and A. T. Beck, *Structural reliability analysis and prediction*, 3rd ed. Hoboken, NJ: John Wiley & Sons Ltd., 2018.

[70] A. M. Hasofer and M. C. Lind, "An exact and invariant first order reliability format," *J. Eng. Mech.*, vol. 100, no. 1, pp. 111–121, 1974.

[71] B. Fiessler, R. Rackwitz, and H. Neumann, "Quadratic limit states in structural reliability," *J. Eng. Mech.*, vol. 105, no. 4, pp. 661–676, 1979.

[72] M. Tichý, "First-order third-moment reliability method," *Struct. Saf.*, vol. 16, no. 3, pp. 189–200, Dec. 1994, doi: 10.1016/0167-4730(94)00021-H.

[73] D. J. Lekou, "Probabilistic design of wind turbine blades," in *Advances in Wind Turbine Blade Design and Materials*, Elsevier, 2013, pp. 325–359.

[74] Y.-G. Zhao and T. Ono, "Moment methods for structural reliability," *Struct. Saf.*, vol. 23, no. 1, pp. 47–75, Jan. 2001, doi: 10.1016/S0167-4730(00)00027-8.

[75] G. Kim, D. Kim, and J. Lee, "Resistance factors for LRFD of laterally loaded drilled shafts in sands characterized for transmission line structures," *J. Geotech. Geoenvironmental Eng.*, vol. 147, no. 5, p. 04021017, May 2021, doi: 10.1061/(ASCE)GT.1943-5606.0002492.

[76] K. K. Phoon, J.-R. Chen, and F. H. Kulhawy, "Probabilistic hyperbolic models for foundation uplift movements," in *Probabilistic Applications in Geotechnical Engineering*, Oct. 2007, pp. 1–12, doi: 10.1061/40914(233)4.

[77] D.-Q. Li, X.-S. Tang, K.-K. Phoon, Y.-F. Chen, and C.-B. Zhou, "Bivariate simulation using copula and its application to probabilistic pile settlement analysis," *Int. J. Numer. Anal. Methods Geomech.*, vol. 37, no. 6, pp. 597–617, Apr. 2013, doi: 10.1002/nag.1112.

[78] J. C. Huffman and A. W. Stuedlein, "Reliability-Based Serviceability Limit State Design of Spread Footings on Aggregate Pier Reinforced Clay," *J. Geotech. Geoenvironmental Eng.*, vol. 140, no. 10, p. 04014055, Oct. 2014,

doi: 10.1061/(ASCE)GT.1943-5606.0001156.

[79] R. B. Nelson, "Introduction," in *An Introduction to Copulas*, 2nd ed., New York, NY: Springer, 2006, pp. 1–5.

[80] A. W. Stuedlein and S. C. Reddy, "Factors affecting the reliability of augered cast-in-place piles in granular soils at the serviceability limit state," *DFI J. - J. Deep Found. Inst.*, vol. 7, no. 2, pp. 46–57, Dec. 2013, doi: 10.1179/dfi.2013.7.2.004.

[81] A. S. Kananyan, "Experimental investigation of the stability of bases of anchor foundations," *Soil Mech. Found. Eng.*, vol. 3, no. 6, pp. 387–392, 1966.

[82] N. C. Consoli, C. A. Ruver, and F. Schnaid, "Uplift performance of anchor plates embedded in cement-stabilized backfill," *J. Geotech. Geoenvironmental Eng.*, vol. 139, no. 3, pp. 511–517, Mar. 2013, doi: 10.1061/(ASCE)GT.1943-5606.0000785.

[83] K.-Y. Gu, N. X. Tran, J. M. Han, K.-S. Kim, K.-W. Ham, and S.-R. Kim, "Centrifuge study on uplift behavior of spread foundation for transmission tower in sand."

[84] Z. Qian, X. Lu, X. Han, and R. Tong, "Interpretation of uplift load tests on belled piers in Gobi gravel," *Can. Geotech. J.*, vol. 52, no. 7, pp. 992–998, 2015, doi: 10.1139/cgj-2014-0075.

[85] W. H. Baker and R. L. Kondner, "Pullout load capacity of a circular earth anchor buried in sand," *Highw. Res. Rec. 108*, pp. 1–10, 1966.

[86] K. Ilamparuthi, E. A. Dickin, and K. Muthukrisnaiah, "Experimental investigation of the uplift behaviour of circular plate anchors embedded in sand," *Can. Geotech. J.*, vol. 39, no. 3, pp. 648–664, 2002, doi: 10.1139/t02-005.

[87] M. Uzielli and P. W. Mayne, "Load-displacement uncertainty of vertically loaded shallow footings on sands and effects on probabilistic settlement estimation," *Georisk Assess. Manag. Risk Eng. Syst. Geohazards*, vol. 6, no. 1, pp. 50–69, Mar. 2012, doi: 10.1080/17499518.2011.626333.

[88] P. W. Mayne and H. G. Poulos, "Approximate displacement influence factors for elastic shallow foundations," *J. Geotech. Geoenvironmental Eng.*, vol. 125, no. 6, pp. 453–460, Jun. 1999, doi: 10.1061/(ASCE)1090-

0241(1999)125:6(453).

[89] KEPCO, “Design standard for transmission tower foundation, DS-1110.” Korea Electric Power Corporation, 2013.

[90] S. Mukherjee and G. L. Sivakumar Babu, “Reliability analysis of anchor foundations Subject to vertical uplift forces,” *Indian Geotech. J.*, vol. 50, no. 6, pp. 982–993, Dec. 2020, doi: 10.1007/s40098-020-00442-2.

[91] MathWorks, “MATLAB R2021A.” MathWorks, Natick, MA, 2021.

[92] D. A. Ratkowsky, “Model Fitting and Uncertainty,” in *Modeling Microbial Responses in Food*, 1st ed., R. C. McKellar and X. Lu, Eds. Boca Raton, FL: CRC Press, 2003, pp. 151–196.

[93] T. W. Anderson and D. A. Darling, “Asymptotic theory of certain ‘goodness of fit’ criteria based on stochastic processes,” *Ann. Math. Stat.*, vol. 23, no. 2, pp. 193–212, Jun. 1952, doi: 10.1214/aoms/1177729437.

[94] K. Lesny, “Probability-based derivation of resistance factors for bearing capacity prediction of shallow foundations under combined loading,” *Georisk Assess. Manag. Risk Eng. Syst. Geohazards*, vol. 13, no. 4, pp. 284–290, 2019, doi: 10.1080/17499518.2019.1633581.

[95] D. M. Zhang, K. K. Phoon, H. W. Huang, and Q. F. Hu, “Characterization of model uncertainty for cantilever deflections in undrained clay,” *J. Geotech. Geoenvironmental Eng.*, vol. 141, no. 1, p. 04014088, 2015, doi: 10.1061/(ASCE)GT.1943-5606.0001205.

[96] A. B. Cerato and A. J. Lutenegger, “Scale effects of shallow foundation bearing capacity on granular material,” *J. Geotech. Geoenvironmental Eng.*, vol. 133, no. 10, pp. 1192–1202, 2007, doi: 10.1061/(ASCE)1090-0241(2007)133:10(1192).

[97] H. Akoglu, “User’s guide to correlation coefficients,” *Turkish J. Emerg. Med.*, vol. 18, no. 3, pp. 91–93, Sep. 2018, doi: 10.1016/j.tjem.2018.08.001.

[98] M. Sadegh, E. Ragno, and A. AghaKouchak, “Multivariate Copula Analysis Toolbox (MvCAT): Describing dependence and underlying uncertainty using a Bayesian framework,” *Water Resour. Res.*, vol. 53, no. 6, pp. 5166–5183, Jun. 2017, doi: 10.1002/2016WR020242.

[99] S. S. Najjar and R. B. Gilbert, “Importance of lower-bound capacities in the design of deep foundations,” *J. Geotech. Geoenvironmental Eng.*, vol. 135,

no. 7, pp. 890–900, Jul. 2009, doi: 10.1061/(ASCE)GT.1943-5606.0000044.

[100] G. B. Baecher and J. T. Christian, "The influence of spatial correlation on the performance of earth structures and foundations," in *GeoCongress 2006*, Feb. 2006, pp. 1–6, doi: 10.1061/40803(187)194.

[101] D. Breysse, "Reliability of a shallow foundation footing," in *Construction Reliability: Safety, Variability and Sustainability*, 1st ed., J. Baroth, F. Schoefs, and D. Breysse, Eds. Hoboken, NJ: John Wiley & Sons, Inc., 2013, pp. 97–117.

[102] X. Chen, D. Li, X. Tang, and Y. Liu, "A three-dimensional large-deformation random finite-element study of landslide runout considering spatially varying soil," *Landslides*, vol. 18, no. 9, pp. 3149–3162, Sep. 2021, doi: 10.1007/s10346-021-01699-1.

[103] H. J. Dagher, *Reliability-based design of utility pole structures*. Reston, VA: American Society of Civil Engineers, 2006.

[104] FHWA, "Load and resistance factor design (LRFD) for highway bridge substructures, FHWA HI-98-032," 2001.

[105] B. R. Ellingwood and P. B. Tekie, "Wind load statistics for probability-based structural design," *J. Struct. Eng.*, vol. 125, no. 4, pp. 453–463, Apr. 1999, doi: 10.1061/(ASCE)0733-9445(1999)125:4(453).

[106] B. Ellingwood, T. V. Galambos, J. G. MacGregor, and C. A. Cornell, "Development of a probability based load criterion for American national standard A58: Building code requirements for minimum design loads in buildings and other structures." National Bureau of Standards, Washington, D.C., 1980.

[107] S. Najjar, E. Shammas, and M. Saad, "A reliability-based approach to the serviceability limit state design of spread footings on granular soil," in *Geotechnical Safety and Reliability*, Jun. 2017, pp. 185–202, doi: 10.1061/9780784480731.016.

[108] A. W. Skempton and D. H. MacDonald, "The allowable settlements of buildings," *Proc. Inst. Civ. Eng.*, vol. 5, no. 6, pp. 727–768, Nov. 1956, doi: 10.1680/ipeds.1956.12202.

[109] G. G. Meyerhof, "Development of geotechnical limit state design," *Can. Geotech. J.*, vol. 32, no. 1, pp. 128–136, Feb. 1995, doi: 10.1139/t95-010.

Appendix A: Load Test Database

Table A.1 Database of uplift load tests on spread foundations under uplift in cohesionless soils

Foundation Type	Test Type	Data No.	Ultimate Capacity Q_u (kN)	Foundation Width B (m)	Embedment Depth D (m)	Foundation Shaft Thickness b (m)	Foundation Slab Thickness t (m)	Embedment Ratio D/B	Foundation Shape	Soil Unit Weight γ_s (kN/m^3)	Friction Angle ϕ (°)
Anchor	Field	K1	20.1	0.40	1.00	0.04	-	2.5	Circular	16.0	32
		K2	24.4	0.60	1.00	0.04	-	1.7	Circular	16.0	32
		K3	31.6	0.80	1.00	0.04	-	1.3	Circular	16.0	32
		K4	39.8	1.00	1.00	0.04	-	1.0	Circular	16.0	32
		K5	51.4	1.20	0.98	0.04	-	0.8	Circular	16.0	32
		S1	2.4	0.30	0.30		-	1.0	Circular	15.8	39
		S2	5.0	0.30	0.45		-	1.5	Circular	15.8	39
		S3	6.8	0.30	0.60		-	2.0	Circular	15.8	39
Footing	Centrifuge	G1	1979.8	3.50	4.55	1.20	0.75	1.1	Square	13.6	37
		G2	2658.1	3.50	5.60	1.20	0.75	1.4	Square	13.6	37
		G3	3615.9	3.50	5.60	1.20	0.75	1.4	Square	15.0	43
		G4	2958.5	4.50	4.50	2.00	1.50	0.7	Square	13.5	37
		G5	3845.0	4.50	5.85	2.00	1.50	1.0	Square	13.5	37
		G6	5351.2	4.50	7.20	2.00	1.50	1.3	Square	13.6	37
		G7	3312.3	4.50	4.50	2.00	1.50	0.7	Square	15.0	43
		G8	4553.6	4.50	5.85	2.00	1.50	1.0	Square	15.1	43

Foundation Type	Test Type	Data No.	Ultimate Capacity Q_u (kN)	Foundation Width B (m)	Embedment Depth D (m)	Foundation Shaft Thickness b (m)	Foundation Slab Thickness t (m)	Embedment Ratio D/B	Foundation Shape	Soil Unit Weight γ_s (kN/m^3)	Friction Angle ϕ (°)
Footing	Centrifuge	G9	7432.7	6.50	6.50	2.00	1.50	0.8	Square	13.6	37
		G10	10440.8	6.50	8.45	2.00	1.50	1.1	Square	13.6	37
		G11	9330.0	6.50	6.50	2.00	1.50	0.8	Square	15.0	43
		G12	12284.2	6.50	8.45	2.00	1.50	1.1	Square	14.9	43
Belled Pier	Field	Q1	450.0	1.01	1.72	0.80	0.20	1.5	Circular	21.7	42
		Q2	1326.0	1.64	2.65	1.20	0.20	1.5	Circular	21.7	42
		Q3	2875.0	2.29	3.64	1.60	0.20	1.5	Circular	21.7	42
		Q4	2349.0	1.41	3.73	1.20	0.20	2.5	Circular	21.7	42
		Q5	6251.0	2.04	5.29	1.60	0.20	2.5	Circular	21.7	42
		Q6	2203.0	1.49	3.93	0.80	0.20	2.5	Circular	21.7	42
		Q7	7428.0	1.81	6.54	1.60	0.20	3.5	Circular	21.7	42
		Q8	3667.0	1.24	4.53	0.80	0.20	3.5	Circular	21.7	42
		Q9	7286.0	1.89	6.82	1.20	0.20	3.5	Circular	21.7	42
		Q10	361.0	1.01	1.72	0.80	0.20	1.5	Circular	21.7	42

Foundation Type	Test Type	Data No.	Ultimate Capacity Q_u (kN)	Foundation Width B (m)	Embedment Depth D (m)	Foundation Shaft Thickness b (m)	Foundation Slab Thickness t (m)	Embedment Ratio D/B	Foundation Shape	Soil Unit Weight γ_s (kN/m^3)	Friction Angle ϕ (°)
Belled Pier	Field	Q11	1097.0	1.64	2.65	1.20	0.20	1.5	Circular	21.7	42
		Q12	3659.0	2.29	3.64	1.60	0.20	1.5	Circular	21.7	42
		Q13	2349.0	1.41	3.73	1.20	0.20	2.5	Circular	21.7	42
		Q14	2768.0	1.49	3.93	0.80	0.20	2.5	Circular	21.7	42
		Q15	3395.0	1.24	4.53	0.80	0.20	3.5	Circular	21.7	42
		Q16	576.0	1.01	1.72	0.80	0.20	1.5	Circular	21.7	42
		Q17	1668.0	1.64	2.65	1.20	0.20	1.5	Circular	21.7	42
		Q18	4524.0	2.29	3.64	1.60	0.20	1.5	Circular	21.7	42
		Q19	3246.0	1.41	3.73	1.20	0.20	2.5	Circular	21.7	42
		Q20	8273.0	2.04	5.29	1.60	0.20	2.5	Circular	21.7	42
		Q21	3211.0	1.49	3.93	0.80	0.20	2.5	Circular	21.7	42
		Q22	8150.0	1.81	6.54	1.60	0.20	3.5	Circular	21.7	42
		Q23	4260.0	1.24	4.53	0.80	0.20	3.5	Circular	21.7	42
		Q24	604.0	1.20	2.05	0.80	0.20	1.5	Circular	21.7	42

Foundation Type	Test Type	Data No.	Ultimate Capacity Q_u (kN)	Foundation Width B (m)	Embedment Depth D (m)	Foundation Shaft Thickness b (m)	Foundation Slab Thickness t (m)	Embedment Ratio D/B	Foundation Shape	Soil Unit Weight γ_s (kN/m^3)	Friction Angle ϕ (°)
Belled Pier	Field	Q25	1155.0	1.23	2.60	0.84	0.20	2.0	Circular	21.7	42
		Q26	1955.0	1.20	3.55	0.80	0.20	2.8	Circular	21.7	42
		Q27	1900.0	1.40	3.20	1.05	0.20	2.1	Circular	21.7	42
		Q28	4522.0	1.60	4.75	1.05	0.20	2.8	Circular	21.7	42
		Q29	3288.0	1.80	4.08	1.25	0.20	2.2	Circular	21.7	42
		Q30	4592.0	1.85	4.80	1.30	0.20	2.5	Circular	21.7	42
		Q31	724.0	1.56	2.54	1.00	0.20	1.5	Circular	21.7	42
		Q32	2129.0	1.36	4.96	0.80	0.20	3.5	Circular	21.7	42
		Q33	761.0	1.12	1.88	0.80	0.20	1.5	Circular	21.7	42
		Q34	904.0	1.56	2.54	1.00	0.20	1.5	Circular	21.7	42
		Q35	2637.0	2.21	3.51	1.20	0.20	1.5	Circular	21.7	42
		Q36	1895.0	1.32	3.50	1.00	0.20	2.5	Circular	21.7	42
		Q37	3300.0	1.76	4.60	1.20	0.20	2.5	Circular	21.7	42
		Q38	3355.0	1.81	4.72	0.80	0.20	2.5	Circular	21.7	42

Foundation Type	Test Type	Data No.	Ultimate Capacity Q_u (kN)	Foundation Width B (m)	Embedment Depth D (m)	Foundation Shaft Thickness b (m)	Foundation Slab Thickness t (m)	Embedment Ratio D/B	Foundation Shape	Soil Unit Weight γ_s (kN/m^3)	Friction Angle ϕ (°)
Belled Pier	Field	Q39	6561.0	1.52	5.53	1.20	0.20	3.5	Circular	21.7	42
		Q40	4228.0	1.36	4.96	0.80	0.20	3.5	Circular	21.7	42
		Q41	2017.0	1.80	4.70	1.20	0.20	2.5	Circular	21.7	42
		Q39	6561.0	1.52	5.53	1.20	0.20	3.5	Circular	21.7	42
		Q40	4228.0	1.36	4.96	0.80	0.20	3.5	Circular	21.7	42
		Q41	2017.0	1.80	4.70	1.20	0.20	2.5	Circular	21.7	42

Appendix B: Convergence Check

To check whether the number of load-displacement curves in the database (N=61) is sufficient for the analysis, a convergence check was carried out. It was checked whether the probability characteristics of the hyperbolic fitting coefficients (θ_1 and θ_2) and the Kendall's tau correlation coefficient (ρ_τ) converge at the sample size of N=61. The convergence check results are shown in Figures B.1-B.3, which display the variation in the parameter values with an increase in the sample size. For demonstration purposes, the samples were inputted randomly in 100 different sequences. As shown in the figures, convergence is reached at the sample size of approximately N=30 – 40. This indicates that the sample size of the database is sufficient for the analysis in this study.

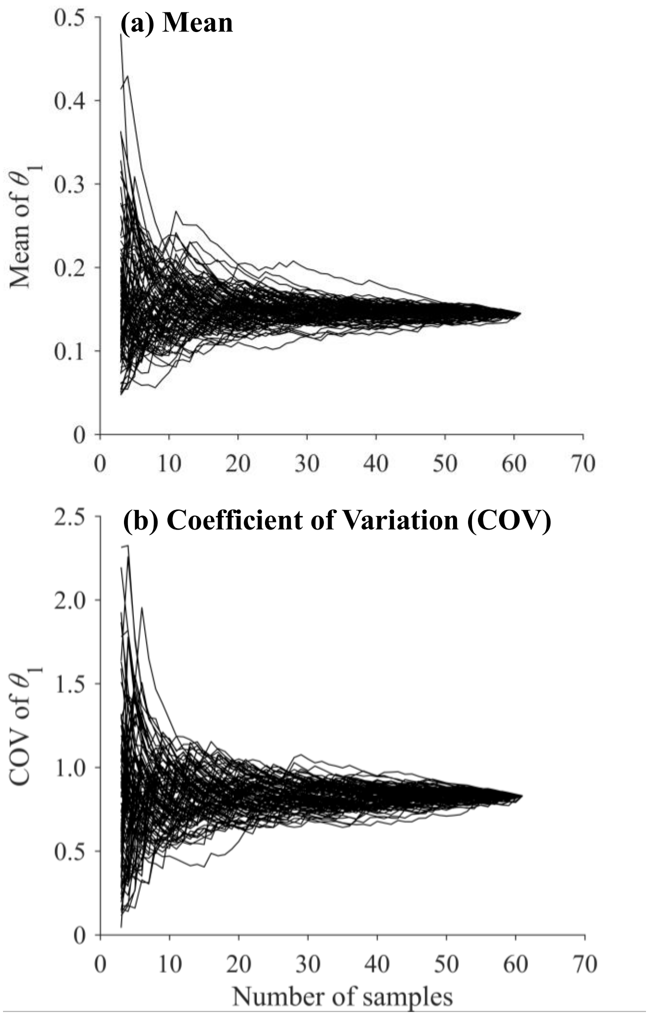

Figure B.1 Convergence check of the probability characteristics of the hyperbolic fitting coefficient θ_1 (Lognormal distribution).

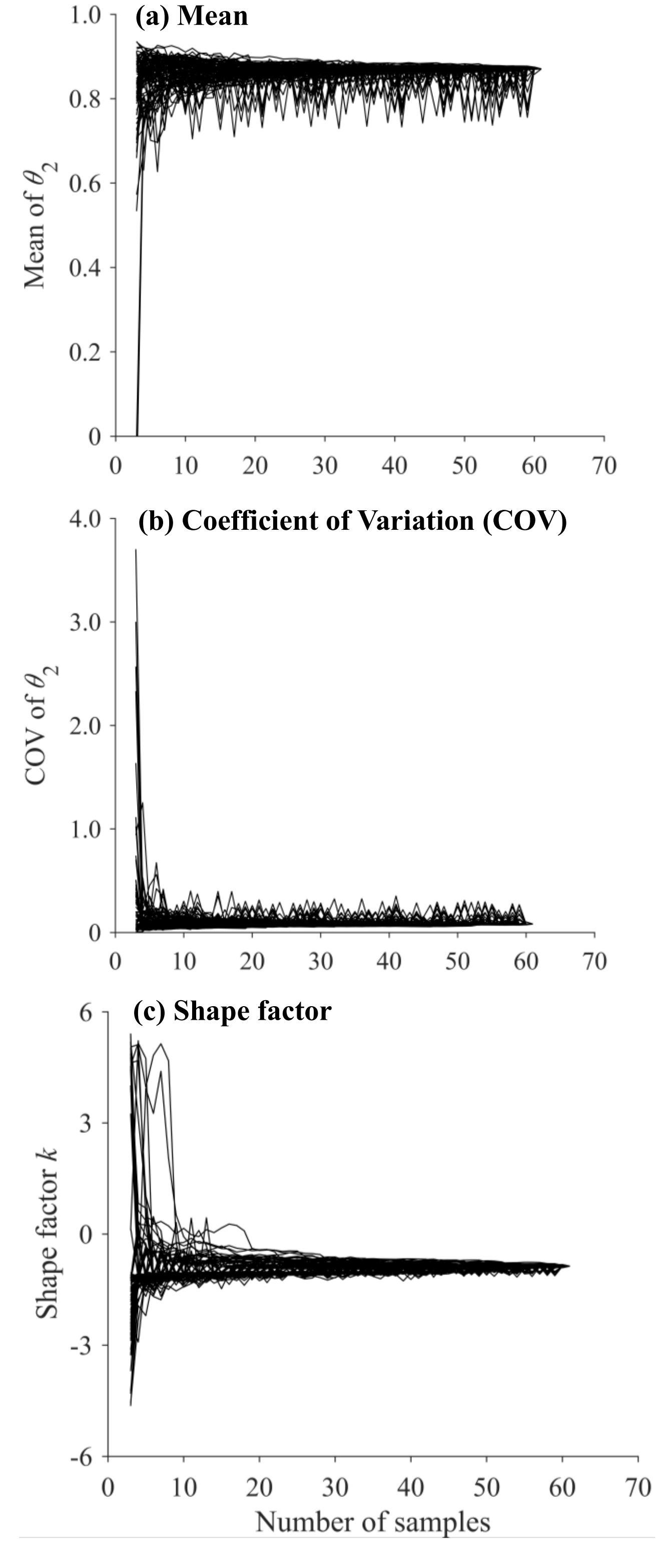

Figure B.2 Convergence check of the probability characteristics of the hyperbolic fitting coefficient θ_2 (Generalised extreme value distribution).

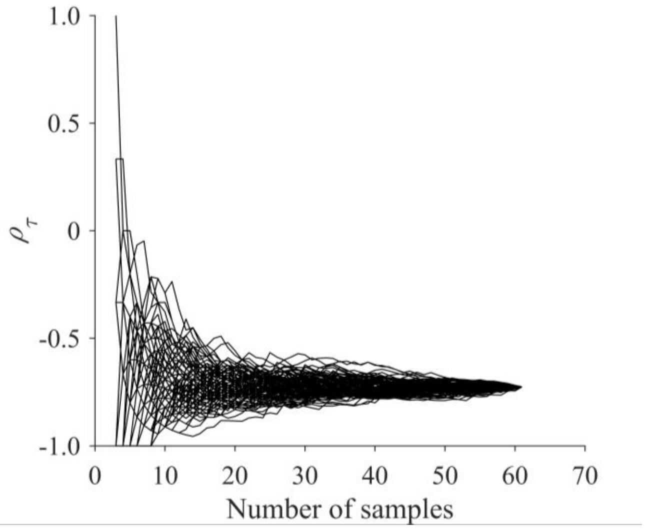

Figure B.3 Convergence check of the Kendall's tau correlation coefficient between the hyperbolic fitting coefficients.

Abstract in Korean

국문 초록

사질토 지반에서 인발하중을 받는 확대기초의 하중-변위 거동의 불확실성을 확률론적 접근을 통해 분석하여, 신뢰성기반 사용성한계상태 설계법을 개발하였다. 하중-변위 곡선을 포함한 기초인발실험 데이터베이스를 구축하여, 각 곡선을 쌍곡선 함수와 멱함수 법칙과 같은 경험적(empirical) 모델로 나타내어 하중-변위 곡선의 통계특성치를 구하였다. 산정한 통계특성치를 활용하여 몬테카를로 시뮬레이션을 통한 신뢰성분석을 진행하고, 사용성한계상태 허용변위에 따른 하중저항계수설계법(LRFD)의 저항계수를 산정하였다. 신뢰성분석 결과, 기초 근입비가 저항계수값에 큰 영향을 주는 것으로 확인되었으며, 하중-거동 곡선의 측정값과 경험적 모델로부터 얻은 예측값 사이의 오차를 반영함으로써, 더 정확한 저항계수값을 산정할 수 있는 것으로 판단되었다. 더 나아가, 사용성한계상태와 극한한계상태 사이의 관계를 분석하여, 허용변위와 목표신뢰도지수에 따른 지배적인 한계상태를 평가하고, 두 한계상태에 대한 동시 파괴가 일어날 확률을 산정하였다. 분석 결과를 토대로, 사용한계상태와 극한한계상태 사이의 관계를 고려한 신뢰성기반 사용성한계상태 설계법을 제시하였다.

주요어: 사용성한계상태; 신뢰성기반 설계; 확대기초; 인발; 기초공학; 하중저항계수설계법; 통계분석

학번: 2021-28916

Acknowledgements

This thesis is derived in part from an article published in *Georisk: Assessment and Management of Risk for Engineered Systems and Geohazards* (Publication date: 9 Jan 2023) Copyright © 2023 Taylor & Francis, available online: https://www.tandfonline.com/10.1080/17499518.2023.2164900